

Geochemical and multivariate statistical study to assess the salinization origin of the Remila plain groundwater, Khenchela Algeria

Type

Research paper

Keywords

salinity, statistics, groundwater, hydrogeochemistry, Remila

Abstract

The aquifer system of the Remila plain 250 km² (Khenchela, Algeria) is one of the semiarid regions where groundwater is heavily exploited for urban supply and irrigation. An integrated hydrogeochemical and statistical approach was performed by 70 water samples to identify the main processes and the origin of our waters' salinization. Chemical analyses indicate salinity values (TDS) ranging from 568 to 1586 mg.l⁻¹ with an average of 869 mg.l⁻¹, sulphate is the dominant ions, especially in the north and northeast part. While the identified chemical facies are : SO₄-Cl-Ca in the northeastern part, SO₄-Cl-Ca-Mg presents most waters and HCO₃-Ca-Mg in the southeastern part. The statistical approach, which allowed us to group the waters into three groups using PCA and HCA; 1) saline waters (23%) (TDS > 1000 mg.l⁻¹ and SO₄²⁻ dominance), 2) moderately saline waters (51%) with HCO₃⁻ dominance, 3) moderately saline waters (26%) with a mixed facies. The binary ion diagrams used suggest that the most hydrochemical processes are: evaporites dissolution and/or precipitation, accompanied by an exchange and/or reverse exchange of ions. Additionally, another process was detected in the northeastern part of the area; the saline intrusion of Sabkha waters, favored by intensive aquifer exploitation.

Explanation letter

Thank you for giving us the opportunity to submit a revised draft of the manuscript "Geochemical and multivariate statistical study to assess the salinization origin of the Remila plain groundwater, Khenchela Algeria" for publication in the Journal of Water and Land Development. We appreciate the time and effort that you and the reviewers dedicated to providing feedback on our manuscript and are grateful for the insightful comments on and valuable improvements to our paper. Attached is a letter in response to the comments of the reviewers with a detailed manuscript description.

Best thanks for your cooperation.

Kindly, cordially,

[Response to Reviewers.docx](#)

1 Geochemical and multivariate statistical study to assess the salinization 2 origin of the Remila plain groundwater, Khenchela Algeria

3 Abstract

4 The aquifer system of the Remila plain 250 km² (Khenchela, Algeria) is one of the semiarid
5 regions where groundwater is heavily exploited for urban supply and irrigation. An integrated
6 hydrogeochemical and statistical approach was performed by 70 water samples to identify the
7 main processes and the origin of our waters' salinization. Chemical analyses indicate salinity
8 values (TDS) ranging from 568 to 1586 mg.l⁻¹ with an average of 869 mg.l⁻¹, sulphate is the
9 dominant ions, especially in the north and northeast part. While the identified chemical facies
10 are : SO₄-Cl-Ca in the northeastern part, SO₄-Cl-Ca-Mg presents most waters and HCO₃-Ca-
11 Mg in the southeastern part.

12 The statistical approach, which allowed us to group the waters into three groups using PCA
13 and HCA; 1) saline waters (23%) (TDS > 1000 mg.l⁻¹ and SO₄²⁻ dominance), 2) moderately
14 saline waters (51%) with HCO₃⁻ dominance, 3) moderately saline waters (26%) with a mixed
15 facies. The binary ion diagrams used suggest that the most hydrochemical processes are:
16 evaporites dissolution and/or precipitation, accompanied by an exchange and/or reverse
17 exchange of ions. Additionally, another process was detected in the northeastern part of the
18 area; the saline intrusion of Sabkha waters, favored by intensive aquifer exploitation.

19 **Keywords:** Groundwater; Hydrogeochemistry; Statistics; Salinity; Remila.

20 1 Introduction

21 Freshwater resources account for only 3% of the planet's water and are mostly in frozen form,
22 where groundwater accounts for only 30% of the world's freshwater [BENCHOKROUN
23 2008; CASSARDO and JONES 2011]. Although groundwater has become an important
24 source of water supply for many countries domestic, industrial and agricultural sectors, and
25 especially in arid and semi-arid regions [PEJMAN *et al.* 2009; BOUZOURRA *et al.* 2015;
26 AOUIDANE 2017b]. In the southern Mediterranean regions, the Maghreb countries have
27 become areas of intensive use of groundwater for agriculture and industry [SIEBERT *et al.*
28 2010]. In Algeria, 67% of irrigated lands are irrigated by groundwater [ZEKTSER and
29 EVERETT 2004]. However, water quality plays a crucial role in plant growth, human health
30 and the environment. Natural processes can lead to deterioration of groundwater quality, and
31 some of these processes are exacerbated by human activities due to the over-exploitation of
32 groundwater resources [RINA *et al.* 2013; MASOUD *et al.* 2018]. The identification of

34 33 geochemical processes in groundwater is, therefore, crucial for the sustainable management of
35 34 these resources.

36 35 Salinization is one of the most common contaminants in water resources, especially in arid
37 36 and semi-arid regions. Indeed, salinization of groundwater is a global concern not only for the
38 37 sustainable exploration of water resources but also for the protection of natural ecosystems
39 38 [PISINARAS *et al.* 2010]. Over the last few decades, salinization of groundwater has been the
40 39 subject of considerable research [GIBBS 1970; YERMANI *et al.* 2003; PAZAND *et al.* 2012;
41 40 AOUIDANE and BELHAMRA 2017a]. This problem can be attributed to natural and/or
42 41 anthropogenic factors, such as; the interaction of water with rocks [FRAPE *et al.* 1984;
43 42 GHESQUIÈRE *et al.* 2015], the intrusion of coastal saltwater or Sabkha water generated by
44 43 excessive groundwater pumping [CAPACCIONIA *et al.* 2005], fossil seawater [TIJANI
45 44 2004; AKOUVI *et al.* 2008; FARID *et al.* 2013]. The anthropogenic intervention finally
46 45 compounded local natural processes by saline water retention due to over-exploitation of
47 46 groundwater, inadequate sewage disposal and intensive agricultural and industrial activities
48 47 [ZEWDU *et al.* 2017]. Generally, groundwater salinization processes can be identified using
49 48 many methods: such as geochemical analysis, with the use binary ratios of major and minor
50 49 tracers [SANCHEZ-MARTOS *et al.* 2002; SCANLON *et al.* 2006; GIL-MÁRQUEZA *et al.*
51 50 2017], Isotopic tracers [CHANGKAKOTI *et al.* 1986; GHABAYEN *et al.* 2006; HASSEN *et*
52 51 *al.* 2016] and including statistical analysis [KHARROUBI *et al.* 2012; VISWANATH *et al.*
53 52 2015; SUDHEER *et al.* 2017; MASOUD *et al.* 2018].

54 53 Like many arid and semi-arid areas, this general situation exists in the endorheic Remila
55 54 basin, which is the subject of this study. Situated in northeastern Algeria, this area is limited
56 55 to the north by the depression of Sabkha Garaat Etarf. Precipitation is rare, characterized by
57 56 sporadic and random temporal and spatial variations, focus on short periods. This area is
58 57 urbanizing with agricultural vocation, and the water supply comes mainly from groundwater.
59 58 Therefore, it is important to understand the main processes that control the salinization of
60 59 these waters, within the limits of improving water resource quality management in this region.
61 60 The main aim of this study is to identify factors that control groundwater salinity. An
62 61 integrated approach between geological, hydrogeological, hydrochemical and statistical was
63 62 used to (1) assessment of groundwater chemistry to highlight dominant groundwater
64 63 mineralization processes (2) use statistical analyzes to identify distinct water groups and
65 64 assess the correlation between different elements and factors of water hydrochemistry (3) and
66 65 identify recharge areas and major sources of contamination. A better understanding of the
67 66 sources of salinization and contamination of the Remila aquifer system (Khenchela) will then

67 serve as an important scientific basis for the study area's water resource planning and
68 management.

69 **2 Materials and Methods**

70 **2.1 Study area**

71 The study area is part of the endorheic basin of Garaat Et Tarf. It is located in northeastern
72 Algeria lies between the parallels 35°25' and 35°40' north latitudes, and 06°30' and 07°05' east
73 longitudes, on an area of 250 km² with a flat topography where an altitude of 800 to 1000 m.
74 The study area is surrounded to the south by the northern slope of the Aurès Mountains,
75 which is the recharge area; to the north by the Djbel Fdjoudj mountain range and to the
76 northeast by the depression Sabkha of Gareat Et Tarf (Fig. 1) [C.P.H. 1977]. The semi-arid
77 climate of the region is characterized by annual precipitation less than 400 mm with an
78 average annual temperature of 17 °C, the minimum and maximum temperatures of which
79 were noted in January (6 °C) and in August (30 °C) respectively and with potential annual
80 evapotranspiration of 1050 mm. Surface water in the area is scarce, and groundwater is the
81 only source of water for urban and agricultural use.

82 **2.1.1 Geological setting**

83 From a geological point of view, the Remila region is located in a depression zone with a
84 length of 50 to 60 km and an average width of 20 km. It represents as a whole, a floodplain of
85 Mio-Pliocene and quaternary deposits transported by Streams, and then deposited in a
86 sequence of floodplains due to stream flow regimes [LAFFITTE 1939; C.G.G. 1969]. The
87 Cretaceous series surrounding the study area is composed of Middle Cretaceous (Aptian) or
88 Upper Cretaceous (Cenomanian, Turonian, and Senonian), which are the most extensive on
89 the south and north side. While in the north-west part, the Miocene is presented by a
90 limestone-sandstone and limestone deposit (Burdigalian) which are arranged discordantly on
91 the Cretaceous and the red Pontian marl. An endorheic saline depression (Sabkha Great Etart)
92 of 200 km² occupies the eastern part of the plain [VILA 1977]. The study area's
93 lithostratigraphy (Remila plain) is characterized by the development of recent Quaternary
94 soils (Fig. 1).

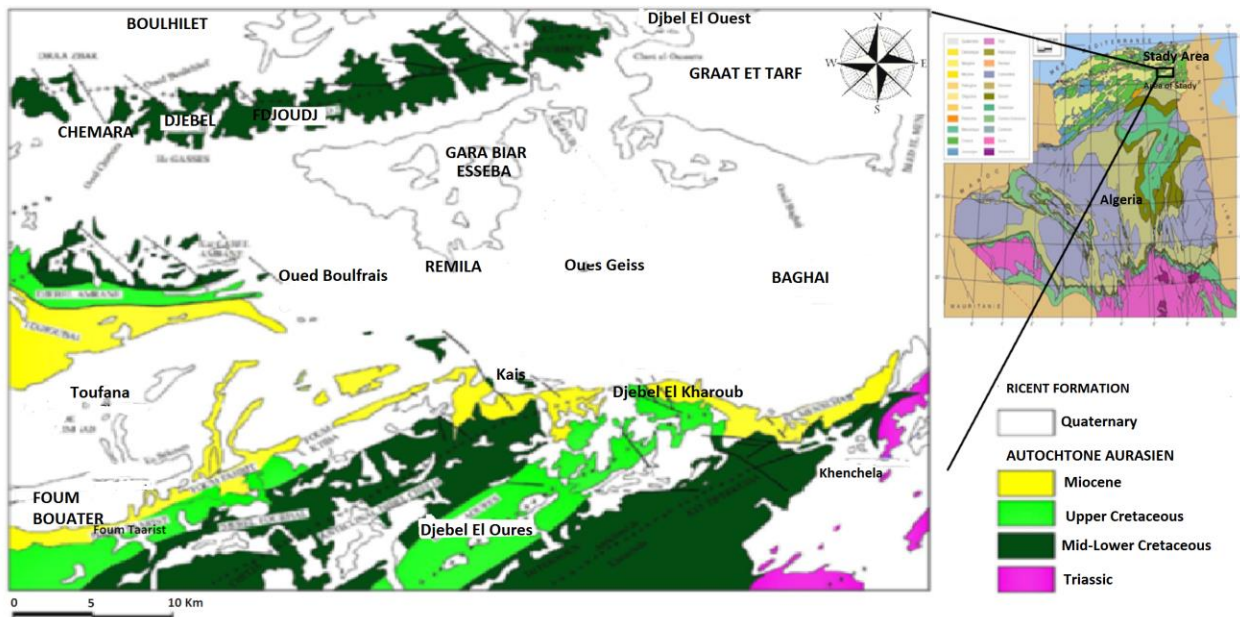


Fig. 1. Map showing location and geological formations of the study area

2.1.2 Hydrogeological setting

The hydrographic system distribution in the study area is related to the evolution of the structural phenomena. The hydrographic network is typified by a significant intensity with a temporary flow during the wet seasons. The Boulefreis Oued drains the entire area from its source to the southwest to discharge to the Sabkha in the northeast. Also, there are other less important streams; the Oued Baghai draining the eastern part, but the center of the area is drained by Oueds Maarouf and Oued Gueiss the streams flow is temporary and pours into a closed depression (Sabkha of Garaat Etarf) [D.H.W.K. 1984].

The Remila aquifer is housed in a sandy-marly limestone substratum of the Moi-Plio-Quaternary. The geochemical properties and groundwater recharge mode will generally depend on the aquifer's depth and lithostratigraphy. Aquifer recharge is maintained through the drainage of runoff water from the northern slope of Aures. The MPQ aquifer is represented by two water tables, housed in the alluvial filling of the plain [C.G.G. 1969]:

- Alluvial aquifers (Plio-Quaternaries): represent the largest regional groundwater resource occupying the Remila basin. They consist of coarse detrital elements, sand, gravel, and conglomerate, packed in a clay-loamy matrix and are the place for good water circulation.
- The Miocene aquifer, which extends along the southern edge of the basin with a synclinal shape defined under the quaternary recovery, is only of local interest and is therefore, less exploited. It's marine sandstone drowned in a large thickness of

121 117 greenish gravelly marls or gray-blue and is actually quite hard and low permeability
122 118 rock.

- 123 119 • The quaternary lands of the western and central plains compose of several gross
124 120 layers, well-developed sand, gravel, and conglomerates. Are less extensive and less
125 121 wide in the southeastern section of the plains. Thus, this formation constitutes a
126 122 permeable cover, allowing meteoric water to infiltrate, which due to its highlighting
127 123 permeability plays an important hydrogeological role.

128 124 2.2 Sample collection

129 125 During two campaigns, groundwater sampling from 35 boreholes was carried out to identify
130 126 the dominant hydrogeochemical processes in the Remila aquifer system. The first is collected
131 127 in the dry period in December-October 2013 and the second is collected in the wet period
132 128 from May-June 2014. We used the methods recommended by RODIER *et al.* [2016] in the
133 129 sampling and analysis to minimize handling errors. Sampling and measurements were carried
134 130 out in functional supply boreholes. The borehole water was pumped out two to three times
135 131 before sampling. Regular monitoring of the electrical conductivity was checked in parallel
136 132 until the values were stable.

137 133 The samples taken from the water are untreated and raw. For each sample, water was taken
138 134 from a 1 liter pre-rinsed polyethylene bottle and filtered through a 0.45 μm membrane filter.
139 135 The bottles were filled to minimize exposure to air, and transported in coolers at 4 °C. The
140 136 sampling point coordinates have been determined using a global geographic positioning
141 137 system (GPS GARMIN Olathe KS, US) (Fig. 2).

142 138 2.3 Sample analysis

143 139 Water physicochemical parameters such as electrical conductivity (EC), TDS (Total
144 140 Dissolved Solids), pH and temperature were measured in situ using a Consort C535
145 141 multiparameter with specific probes, which had been pre-calibrated in the laboratory. Also,
146 142 the dosage of the other parameters was conducted at Constantine University, Algeria, in the
147 143 hydrochemical laboratory (Tab. 1).

148 144 **Table 1.** Methods used for major ion and isotope analysis in the waters of Remila

149 Elements	149 Methods of analysis
150 Ca^{2+} and Na^+	150 Industrial flame photometers PFP7
151 Mg^{2+} , K^+ , Sr^{2+} , Al^{3+} and Li^+	151 Perkin Elmer atomic absorption AA 200 (FXAA)
152 SO_4^{2-} and NO_3^-	152 Colorimetric method
153 Cl^- and HCO_3^-	153 Volumetric method

Multivariate statistical analysis of the data was one of the methods used to analyze geochemical data, allowing to reduce the large dataset of variables to a few factors to elucidate correlations between chemical parameters. Our statistical analysis of the data was carried out using STATISTICA 7.1 (StatSoft1) software. Principal Component Analysis (PCA), Correlation Table, and Hierarchical Clustering Analysis (HCA) were applied in our case.

3 Resultants and Discussion

3.1 General hydrochemical features

3.1.1 Spatial distribution of groundwater salinity

The results of the groundwater physicochemical analysis are given in Tab. 2. Salinity is one of the most important water-classification parameters, Where our water's salinity values (TDS) range from 568 to 1586 mg.l⁻¹, and with an average of 906.3 mg.l⁻¹, this suggests low to medium mineralization of water during the dries season. While the TDS values in the wet season ranged from 1250 to 3270 mg.l⁻¹ with an average of 1822.16 mg.l⁻¹, our waters raise from medium to high mineralization. After the wet season we notice the significant increase in the salt charge, it suggests that the rainwater that feeds the groundwater influences the mineralization of our waters. While the pH values of the majority of the points are close to neutrality where they are between 6.5 and 7 and an average of 6.9 during the wet period, while the values oscillate between 6.5 and 7.21 and an average of 6.91 during the dry period, this indicates a slight seasonal variation.

Table 2 Descriptive statistics of Remila water parameters (mg.l⁻¹)

	Campaign	Mean	Median	Minimum	Maximum	Std.Dev.	Coef.Var.	Skewness	Kurtosis
pH	Dry period	6.87	6.92	6.52	7.02	0.13	1.90	-1.51	1.33
	Wet period	6.91	6.92	6.50	7.21	0.11	1.55	-1.27	7.09
TDS	Dry period	896.29	824.50	568.00	1586.00	254.52	28.40	1.29	1.13
	Wet period	1797.14	1710.00	1250.00	3270.00	485.57	27.02	1.67	2.87
Ca²⁺	Dry period	134.74	132.26	40.08	252.50	39.36	29.21	0.49	2.41
	Wet period	132.14	128.26	44.09	248.50	46.42	35.13	0.76	1.18
Mg²⁺	Dry period	50.83	35.88	6.96	239.64	53.54	105.34	2.63	6.50
	Wet period	56.83	52.68	28.80	129.48	22.48	39.55	2.04	4.59
Na⁺	Dry period	55.56	41.75	11.96	145.59	34.78	62.61	1.45	1.49
	Wet period	69.46	62.11	29.67	162.15	33.45	48.16	0.93	0.41
K⁺	Dry period	1.09	0.17	0.02	9.98	2.09	191.45	2.94	9.57
	Wet period	1.16	1.00	0.09	3.95	0.80	69.13	1.87	4.43
HCO₃⁻	Dry period	174.75	164.70	54.90	280.60	53.64	30.70	0.31	-0.30

	Wet period	253.20	256.20	183.00	402.60	48.86	19.30	0.96	1.39
Cl ⁻	Dry period	122.80	118.93	35.50	312.40	58.36	47.53	1.16	2.07
	Wet period	125.79	117.15	35.50	333.70	83.41	66.31	1.22	0.90
SO ₄ ²⁻	Dry period	344.24	320.00	160.00	704.00	129.92	37.74	1.64	2.84
	Wet period	293.86	270.00	140.00	1250.00	188.44	64.13	4.05	20.20
NO ₃ ⁻	Dry period	-	-	-	-	-	-	-	-
	Wet period	8.19	3.60	0.20	39.00	11.09	135.45	1.96	2.42

Std.Dev: Standard Deviation; Coef.Var: Coefficient of variation.

The results of 35 points have led to generating a spatial distribution map of salinity (TDS) (Fig. 2). We note that the piezometric map of groundwater presents a rather close resemblance, reflecting changes in the mineralization of the water, upstream to downstream (south to north), although some specific trends are also apparent. This spatial variation is classifiable into two water types: the waters of the southern and western parts of the plain are low salty and the waters of the northern part near the Sabkha are moderately salty. This is possibly due to the massive influence of Sabkha's salt waters.

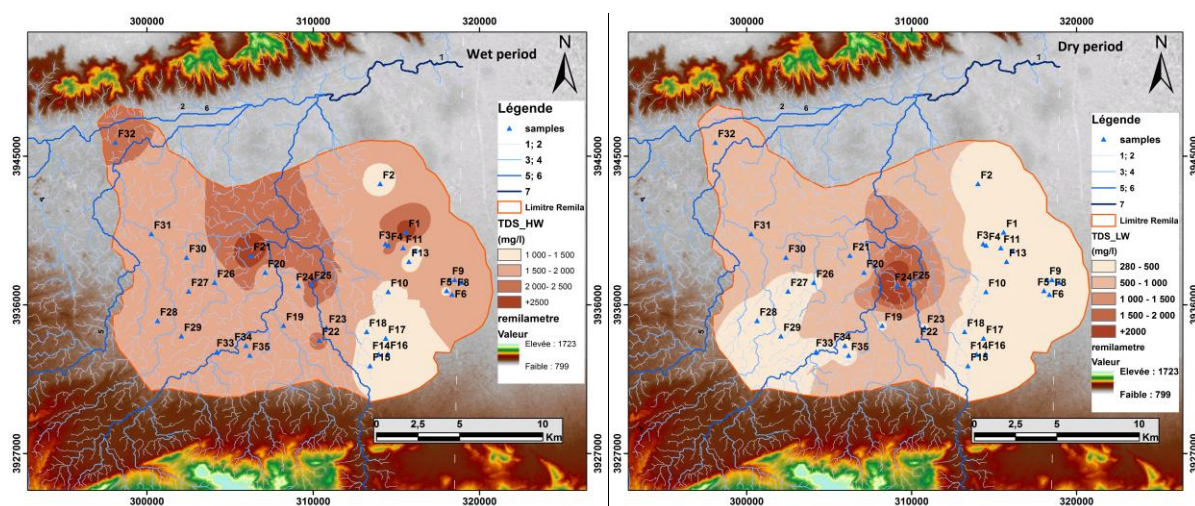
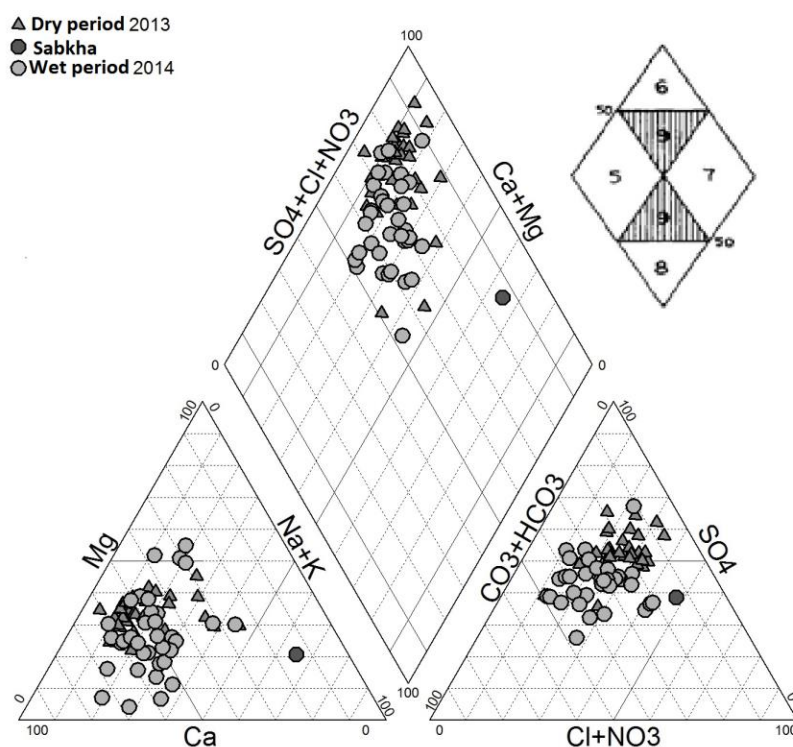


Fig. 2. Spatial salinity distribution map (TDS) of groundwater Remila (Khenchela)

3.1.1 Hydrochemical facies

Identifying the hydrochemical type of water is a useful tool for assessing water chemistry and processes such as mixing, cation exchange, and dissolution that affect the composition of groundwater. The Piper diagram [PIPER 1944] is considered to be the common method of performing multiple analyzes on the same graph. It allows for grouping samples and defining the various groundwater origins [WALTON 1965]. The main ionic species obtained from the geochemical analysis of 70 samples are projected on the piper diagram using DIAGRAMS 5.1 software [SIMLER 2012] (Fig. 3). On the bases of the results, we will deduce the dominance of three chemical facies in our waters, and this in the two companions (dry period

213 185 and wet period) : $\text{SO}_4\text{-Cl-Ca}$ saltwater presented by certain points in the north-eastern part of
214 186 the area near Sabkha, $\text{SO}_4\text{-Cl-Ca-Mg}$ moderately saline waters presented by the majority of
215 187 points and the good quality type $\text{HCO}_3\text{-Ca-Mg}$ presented by some points in the southeastern
216 188 part of the area.
217 189 Most of the water points show a tendency for SO_4^{2-} dominance in the anionic triangle,
218 190 especially samples taken after the wet season, while in the cationic triangle there is a tendency
219 191 towards Ca^{2+} domination. This suggests that the aquifer is affected by different hydrochemical
220 192 processes: ionic exchange with the substratum, leaching and dissolution of sediments in the
221 193 southern part (Recharge areas after a wet season) and saltwater intrusion of the Sabkha waters
222 194 in the northeastern regions.



223 195
224 196 **Fig. 3.** Piper diagram of Remila groundwater (Dry period and Wet period).

225 197 **3.2 Statistical Analysis**

226 198 Descriptive statistical evaluation of data is a critical step in any statistical analysis (Tab. 2)
227 199 [YANG *et al.* 2011; HOSSEINI *et al.* 2014]. The measured parameter values are
228 200 characterized by very high variance. The most important factor that can describe the
229 201 variability of the water parameter values is the variance coefficient (VC). A low variance
230 202 coefficient (<10 %) for pH was calculated suggesting a low spatial variability in the study
231 203 area. While for the TDS, HCO_3^- , Ca^{2+} , and Fe^{2+} , a moderate coefficient of variance (20-50 %)

was observed, indicates moderate spatial variability for these parameters, and is mainly influenced by natural factors. Nonetheless, for Mg^{2+} , Na^+ , K^+ , SO_4^{2-} , Cl^- and NO_3^- , very high CV values exceeding 50% were observed, suggesting a very high spatial variability and these parameters are affected by natural and anthropogenic factors.

The Skewness reflects the symmetric distribution when these values are under 0 the totality of the data is below the average. For the data to have a normal distribution, the skewness value equals zero [GALVAO *et al.* 2013; BROVELLI *et al.* 2011]. The calculated skewness values of Ca^{2+} , Na^+ , and HCO_3^- are close to zero indicate that the data follow a normal distribution. However, other parameters have values >1 , this does not require a data transformation. OLIVER *et al.* [2002], KERRY and OLIVIER [2007] and OLIVER [2010] have shown that Skewness values outside the ± 1 standard limits envelope do not necessarily imply the need to transform the data into statistics for further study, especially when the data values were high.

3.2.1 Pearson's correlation matrix

Many significant correlations between the different ions were established using the correlation matrix of the various parameters (Table 3). A strong correlation ($r > 0.7$) was found between the chemical tracers SO_4^{2-} , Cl^- , Mg^{2+} , Na^+ , Ca^{2+} , Sr^{2+} and total dissolved solids (TDS), indicating an evaporite origin (from $NaCl$, $CaSO_4$, $CaSO_4 \cdot 2H_2O$, $MgSO_4$ or $SrSO_4$) of these elements in the water. However, this is not the case for HCO_3^- which has a low correlation with the salinity indicator TDS, which is explained by its low concentration in the water solution that ranges between 54.9 to 280.6 mg.l⁻¹. Besides, the correlation coefficients between chloride ($r = 0.81$) and sodium ($r = 0.81$), with the (TDS), suggests the same origin for these two elements. On the other side, there is a slight difference between sulfate ($r=0.95$), magnesium ($r=0.87$) and calcium ($r=0.66$) correlation coefficients with TDS, Can be explained by the unconservative transport of calcium and magnesium ions (cation exchange with clay minerals which are most abundant in the area and/or participate in precipitation/dissolution reactions) [VAN BREUKELEN *et al.* 1998].

Concerning the relationship between anions and cations, significant correlations were found between Cl^- and Na^+ ($r=0.55$), Cl^- and Ca^{2+} ($r= 0.74$), Cl^- and Mg^{2+} ($r=0.68$), Cl^- and K^+ ($r=0.65$), SO_4^{2-} and Mg^{2+} ($r=0.93$), SO_4^{2-} and Ca^{2+} ($r=0.61$). This tends to prove that most chloride comes from the dissolution of KCl and $NaCl$ but a very small proportion of this anion could come from the dissolution of other minerals. The low correlation between chloride and sodium can be explained by the involvement of sodium ions in cation exchange with the clay substratum of the aquifer. Additionally, there was a relatively significant correlation between Cl^- with Ca^{2+} (0.74) and Cl^- with Mg^{2+} (0.68). This is due to the water

238 salinity that is caused by several processes that characterize the highly mineralized waters,
239 including an exchange of cations and dissolution of gypsum and halite that can increase the
240 concentrations of calcium, magnesium, and chloride, respectively.

241 **Table 3.** Correlation matrix of different groundwater parameters (mg.l⁻¹)

Variable	pH	TDS	Ca	Mg	Na	K	HCO ₃	Cl	SO ₄	Fe	Mn	Sr
pH	1.00											
TDS	0.16	1.00										
Ca	0.22	<u>0.66</u>	1.00									
Mg	0.26	<u>0.87</u>	0.43	1.00								
Na	0.00	<u>0.81</u>	0.17	<u>0.69</u>	1.00							
K	0.16	<u>0.82</u>	0.38	<u>0.79</u>	<u>0.75</u>	1.00						
HCO ₃	-0.33	0.20	-0.14	-0.02	0.44	0.14	1.00					
Cl	0.31	<u>0.81</u>	<u>0.74</u>	<u>0.68</u>	<u>0.55</u>	<u>0.65</u>	-0.18	1.00				
SO ₄	0.19	<u>0.96</u>	<u>0.61</u>	<u>0.93</u>	<u>0.74</u>	<u>0.80</u>	0.02	<u>0.73</u>	1.00			
Fe	-0.08	0.21	0.28	0.15	0.00	0.20	0.08	0.16	0.20	1.00		
Mn	0.01	-0.24	-0.36	-0.21	-0.05	-0.12	0.24	-0.44	-0.22	-0.07	1.00	
Sr	-0.01	<u>0.71</u>	<u>0.58</u>	<u>0.57</u>	0.45	0.62	0.34	0.46	<u>0.66</u>	0.36	-0.04	1.00

242 We carried out the main component analysis (PCA) and hierarchical clustering analysis
243 (HCA) using the software STATISTICA 8 [STATSOFT 2010] in an attempt to clarify the
244 relationship between the chemical elements (variables) and grouping water points
245 (individuals) with the same chemistry.

246 3.2.2 Principal component analysis (PCA)

247 More and more studies are based on statistical analysis to define water types; one of the most
248 recommended approaches is the principal component analysis [FARNHAM *et al.* 2003 in
249 OLIVIER 2015; AYADI *et al.* 2018]. In the Remila aquifer samples, the variable factors F1-
250 F2 (Fig. 4(a)) (Table 4) show that this plan expresses 53.95% of the expressed variance. The
251 factor F1 (36.74%) is negatively determined by the majority of the elements: TDS, SO₄²⁻, Cl,
252 Mg²⁺, K⁺, Na⁺, and Ca²⁺ and therefore has a mineralization axis of evaporites and salinity. A
253 very good correlation exists between TDS, SO₄²⁻ and Mg²⁺. The F2 explains 17.21% of the
254 total variance, which is positively associated with pH and HCO₃⁻, suggesting that the
255 dissolution of carbonates does not contribute to the mineralization of water.

256 The projection results variables and individuals in the factorial plan (F1, F2) shown in Fig.
257 4(a), allow nodes identifies three different water groups. The first type (I) are saline waters

258 presents with (23%), where TDS exceeds 1000 mg.l-1 and which are characterized by a high
 259 concentration of SO_4^{2-} , Type (II) are non-saline water presents (51%) waters with high
 260 concentrations of HCO_3^- and Type (III) is moderately saline waters with mixed facies presents
 261 in the eastern part of the region with (26%).

262 **Table 4.** Varimax factor loading matrix, communalities for each variable analyzed

Parameters	Factor 1	Factor 2	Factor 3	Factor 4	Factor 5
pH	-0.2245	-0.5564	0.4408	0.1886	-0.2360
TDS	-0.9795	0.0831	0.0054	-0.0857	0.0711
Ca	-0.6711	-0.3059	-0.4608	0.0097	-0.2072
Mg	-0.8954	-0.0599	0.2170	0.0042	0.0861
Na	-0.7563	0.3892	0.3325	-0.1522	0.2471
K	-0.8628	0.1267	0.1683	-0.0418	0.0688
HCO_3	-0.0889	0.8501	-0.0524	-0.0639	0.2252
Cl	-0.8338	-0.3110	-0.0842	-0.0693	-0.0157
SO_4	-0.9552	-0.0205	0.0742	-0.0525	0.0339
Fe	-0.2704	0.0499	-0.5723	0.5659	0.1012
Mn	0.2749	0.4881	0.4029	0.2935	-0.3649
Sr	-0.7282	0.3298	-0.3126	0.1030	-0.1388

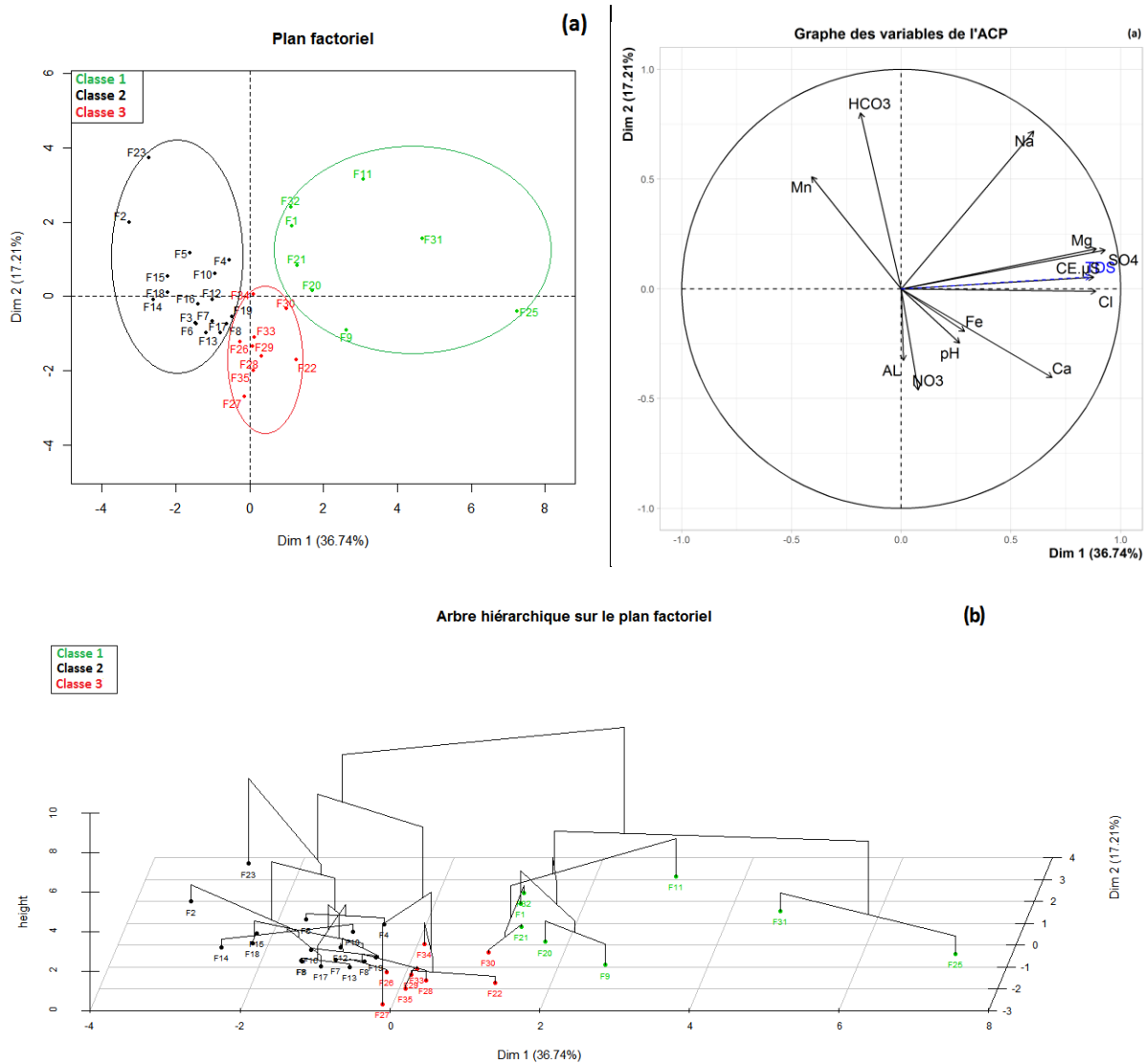
3.2.3 Hierarchical cluster analysis (HCA)

265 The ascending hierarchical clustering (AHC) is a powerful multivariate statistical technique to
 266 analyze water chemistry data for geochemical model formulation [YIDANA 2008; AHOUSSE
 267 *et al.* 2011].

268 The results from the analysis of the hierarchical ascending data classification can be observed
 269 in the dendrogram using the Euclidean distance for similarity measures (Fig. 4(b)), highlights
 270 three principal groupings of the variables. The first group includes the individus (waters
 271 points): he first group is that of waters occupying the north-western part of the area, are salty
 272 waters characterized by a dominance of SO_4 , the second group that presents the majority of
 273 waters in the eastern and south-eastern part of the region, characterized by low salinity with a
 274 mixed face, in the last group, the waters of the south-western part are moderately saline with a
 275 dominance of HCO_3 .

276 The results provided by the PCA of the individual samples and ascending hierarchical
 277 clustering are in the perfect agreement since they demonstrated that water mineralization is

336 278 dominated by sulfate. Besides, the typology of the water samples can be represented by three
 337 279 facies.



338 280

339 281

340 282 **Fig. 4.** Statistic analysis; (a) Principal component analysis, (b) the Ascending hierarchical
 341 283 clustering of Remila waters (Khenchela)

342 284 **3.3 Groundwater mineralization processes**

343 285 Correlations show a statistical relationship between two variables or more. Our results
 344 286 confirm a significant correlation between SO₄²⁻, Mg²⁺, Cl⁻, Ca²⁺, Na⁺, HCO₃⁻, Sr²⁺, K⁺, and
 345 287 TDS, indicate the contribution of these elements to the salinity of the groundwater and
 346 288 suggest that a common source of mineralization may be the dissolution of the evaporitic
 347 289 rocks. Such results require geochemical calculations of speciation-solubility in order to
 348 290 identify the dominant processes, which influence the Remila plain groundwater
 349 291 hydrogeochemistry.

350

3.3.1 Water-rock interaction

To assess the water-rock interaction processes, diagrams ion ratio of $\text{Ca}^{2+}/\text{Na}^+$ versus $\text{HCO}_3^-/\text{Na}^+$ and $\text{Ca}^{2+}/\text{Na}^+$ versus $\text{Mg}^{2+}/\text{Na}^+$ were used to identify the influence of silicate weathering, dissolution evaporites and carbonate alteration on mineralization of groundwater in the study area. The projection results of the water points (Fig. 5(a)), infer that the bulk of the waters are affected by silicate weathering with a bent towards carbonate dissolution, especially after the wet period. The spatial distribution suggests that the waters near the limestone formations of the eastern part are more or less influenced by carbonate dissolution, whereas the waters of the northwestern part are affected by silicate alteration. The normalization of Na by intake Ca versus Mg (Fig. 5(b)), indicates that the bulk of Mg within the waters of the Eastern part is released by carbonate dissolution, in contrast, the Mg within the waters of the western part are influenced by silicate weathering. The $\text{Ca}^{2+}/\text{Mg}^{2+}$ ionic ratio is widely used to identify the dissolution of calcite and dolomite, when the ratio values are ≤ 1 indicates the dominance of the dissolution of dolomite, if the values are between 1 and 2 indicates the dominance the dissolution of calcite and cons if the values are ≥ 2 waters are affected by silicate minerals [SRINIVASAMOORTHY *et al.* 2014; SINGH *et al.* 2017]. The ratio calculation outcomes suggest that, the waters in the extreme south are dominated by means of dolomite dissolution, the majority of the waters in the primary central part of the area are dominated by calcite dissolution, whilst the northern part is affected with silicate weathering.

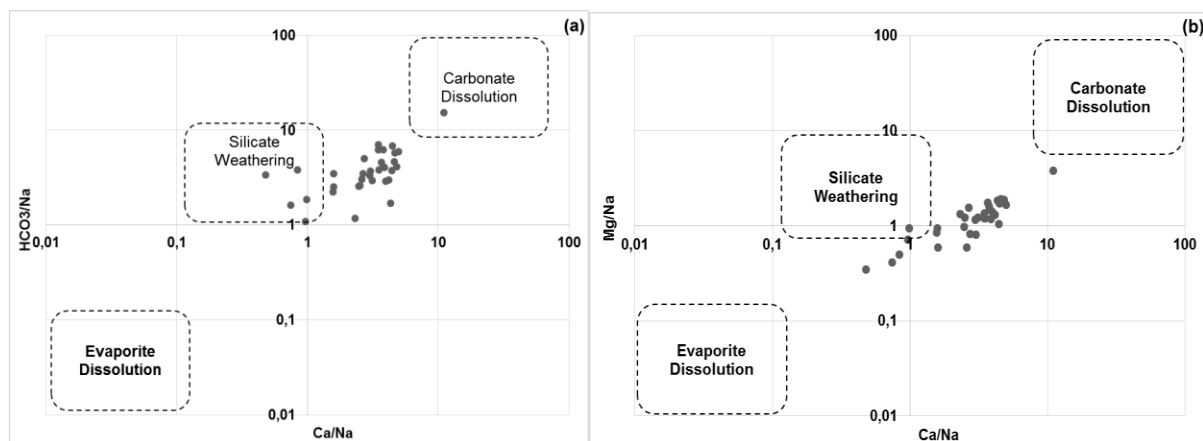


Fig. 5. Scatter plots of a) $\text{Ca}^{2+}/\text{Na}^+$ versus $\text{HCO}_3^-/\text{Na}^+$, b) $\text{Ca}^{2+}/\text{Na}^+$ versus $\text{Mg}^{2+}/\text{Na}^+$ ratio of the Remila groundwater samples

The Gibbs diagrams (GIBBS 1970) are widely used to assess the functional source of ions dissolved in water such as; dominance of precipitation, weathering of rocks and dominance of evaporation which controls the water chemistry (SINGH *et al.* 2011; VAROL and DAVRAZ 2014; MASOUD *et al.* 2018). The chemical data are plotted in a semi-logarithmic dispersion

of TDS values versus anion ($Cl/(Cl+HCO_3^-)$) and cations ($Na^+/(Ca^{2+}+Na^+)$) ratios, where all concentrations Ionic values are expressed in $meq.l^{-1}$ (Fig. 6 (a, b)).

As shown by the data projected in the Gibbs diagrams, the majority of the groundwater samples of the two seasons are located in the predominantly rocky zone, but also have a tendency towards the zone of evaporation and precipitation. The mineralization of our waters is therefore controlled by the dissolution of evaporitic rocks and is also affected by the waters of Sabkha, which are exposed to intense evaporation with chemical precipitation of minerals, which increases the salinization of our waters, particularly in the northeastern part of the area.

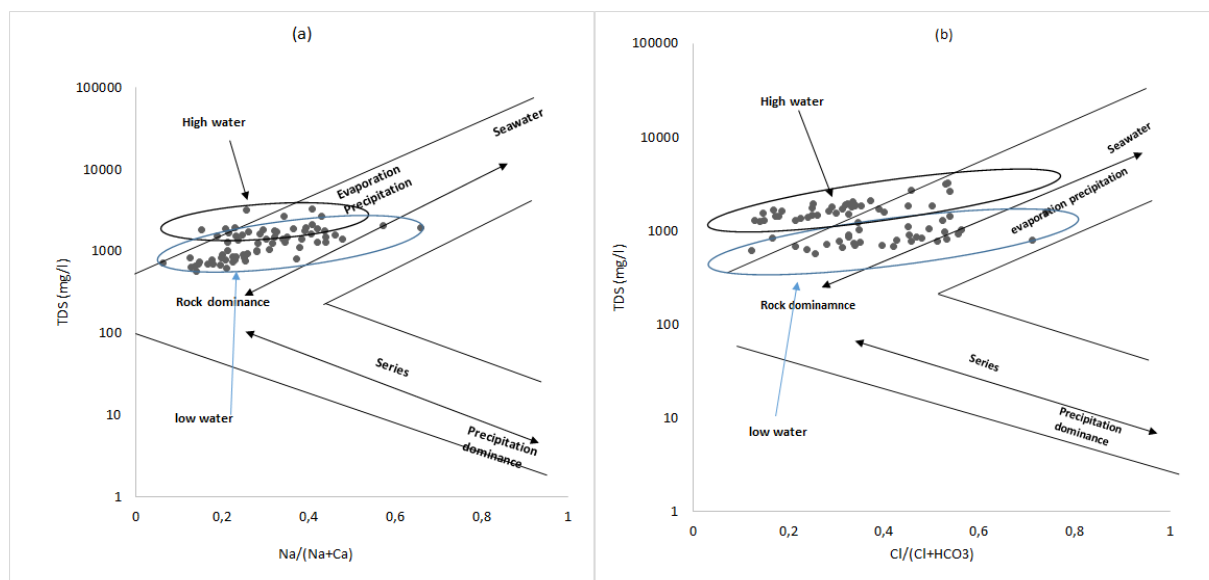


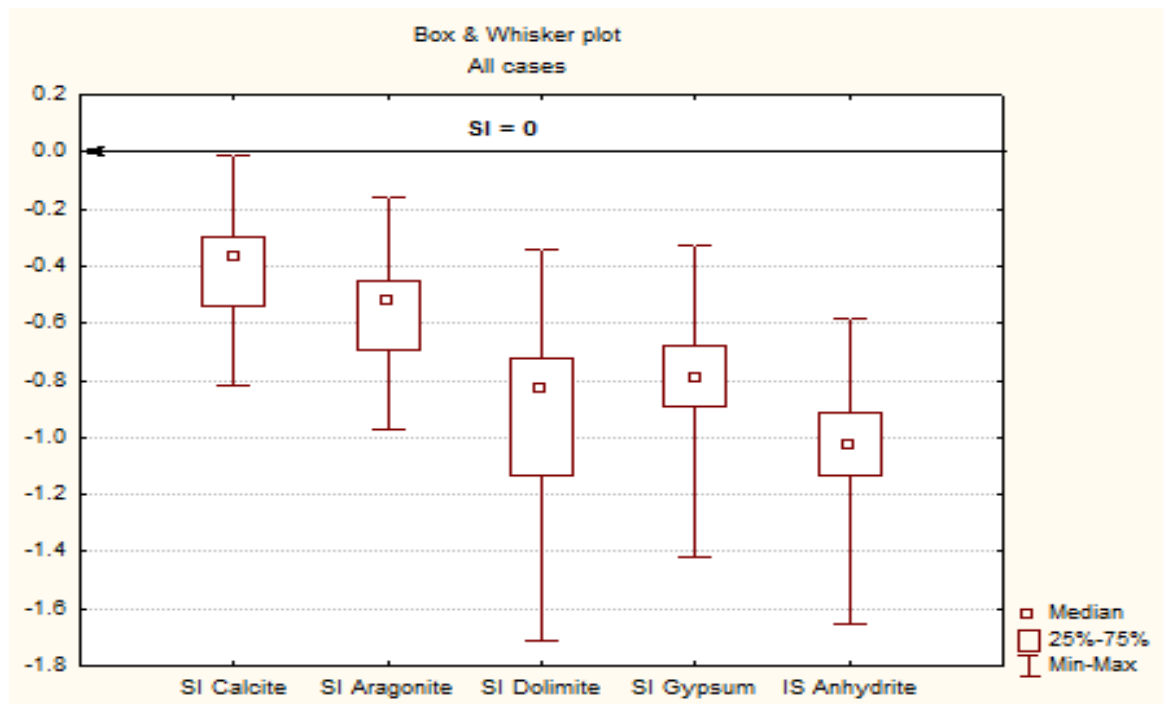
Fig. 6. Gibbs diagrams of Remila groundwater

Another index is commonly used to identify water-rock interactions, as well as hydrochemical processes affecting groundwater chemistry [PLUMMER *et al.* 1976; DAVID *et al.* 1999; KUMARI *et al.* 2013; AYADI *et al.* 2018]. The saturation index (SI) describes the level of saturation of the water towards the various minerals; when $SI = 0$, the minerals in the aqueous solution are in equilibrium; when $SI < 0$, the minerals of the aqueous solution are under saturated which contribute to the dissolution of the minerals, while $SI > 0$ indicates a saturation of solution will contribute to the precipitation of the minerals [APPELO and POSTMA 1994]. The mineral saturation index was calculated using the PHREEQC geochemical modeling program, using the following equation (GARRELS and MACKENZIE 1967):

$$SI = \log\left(\frac{IAP}{K_t}\right) \quad (1)$$

SI: Saturation Index

401 340 IAP : Ion activity product
402 341 K_t : The equilibrium solubility constant
403 342 Results showing that the area's groundwater is under-saturated with respect to gypsum,
404 343 anhydrite, and dolomite ($SI < 0$) indicate that these minerals should be dissolved in our water.
405 344 While groundwater is slightly under-saturated with calcite and aragonite, this means it has
406 345 some equilibrium with these minerals, but these minerals may have influenced the chemical
407 346 composition of the water (Fig. 7).



408 347
409 348 **Fig. 7.** Saturation index (SI) variability diagrams in groundwater at Remila (Khenchela)

410 349 3.3.2 Cationic exchange

411 350 Most of the results show an excess concentration of cations by anion supply, which indicates
412 351 that another source of these cations should be possible, such as exchange. Nevertheless,
413 352 SCHOELLER'S [1965] proposed chloroalkaline index (CAI) can be used to determine the
414 353 degree of ion exchange reactions between the aquifer substratum and groundwater. It is a
415 354 commonly used tool for recognition of dominant processes of ion exchange in groundwater
416 355 [AYADI *et al.* 2018; ABU-ALNAEEM *et al.* 2018]. The CAI is calculated using the equation
417 356 $(Cl^-(Na^++K^+))/Cl^-$ where the values are in $meq.l^{-1}$. If the CAI values tend to decrease
418 357 (negative), indicates a dominance of the basic processes of ion exchange, where Ca^{2+} and
419 358 Mg^{2+} are adsorbed on the substratum and K^+ and Na^+ are released in water. Thus, if the CAI
420 359 index values tend to increase (positive), this implies a dominance of the processes of reverse
421 360 ion exchange, where K^+ and Na^+ are adsorbed on the substratum and Ca^{2+} and Mg^{2+} are

423 361 released in water. While if the CAI values are close to zero show a balance, this implies the
424 362 absence of an exchange process.

425 363 The calculated chloro-alkaline index in the study area shows positive values for most
426 364 groundwater samples (68%), which indicates the dominance of the reverse exchange process
427 365 in which Ca^{2+} , Mg^{2+} of the aquifer substratum is released and Na^+ , K^+ are adsorbed. Although
428 366 26% of the samples have values close to zero, which imply an equilibrium, indicates an
429 367 absence of ion exchange, they are found in the southeastern part of the region. Nevertheless,
430 368 only 2% of the samples show negative values, which indicates the dominance of the processes
431 369 of direct ion exchange, thus releasing Na^+ , K^+ from the aquifer substratum and fixing Ca^{2+} ,
432 370 Mg^{2+} from the water, they are found in the northeastern part of the region.

433 371 Wide fluctuations in the concentration of major ions occur by various processes, ion exchange
434 372 often causes changes or reversals of groundwater cationic concentrations. Studying the
435 373 relationship between $(\text{Ca}^{2+}+\text{Mg}^{2+})$ and $(\text{HCO}_3^-+\text{SO}_4^{2-})$ will however allow us to identify the
436 374 processes that influence groundwater mineralization. The binary diagram of $(\text{Ca}^{2+}+\text{Mg}^{2+})$
437 375 versus $(\text{HCO}_3^- + \text{SO}_4^{2-})$ (Fig. 8 (a)) shows a projection of the water points around the line
438 376 (1:1). Generally, the water points, which are close or on the line (1:1), are under the influence
439 377 of the dissolution of calcite, dolomite, anhydrite, and gypsum [HAMZAOUI-AZAZA *et al.*
440 378 2012; HASSEN *et al.* 2016]. While the water points that exist above the line (1:1), present an
441 379 excess of $(\text{Ca}^{2+}+\text{Mg}^{2+})$ that are accompanied by ion exchange [TLILI-ZRELLI *et al.* 2013].
442 380 On the other hand, the water points located below the line (1:1), have a deficit in
443 381 $(\text{Ca}^{2+}+\text{Mg}^{2+})$; this decrease in concentration is due to reverse ion exchange [RINA *et al.*
444 382 2013]. The result of the water points projection in the diagram (Fig. 8(a)) shows that most
445 383 waters are above line (1:1) due to excess $(\text{Ca}^{2+}+\text{Mg}^{2+})$ and this indicates that reverse ion
446 384 exchange is a very abundant geochemical process in the region. The water points located in
447 385 the northeastern part near Sabkha (saltwater) are projected below the line (1:1), suggesting a
448 386 deficit in $(\text{Ca}^{2+}+\text{Mg}^{2+})$, which indicates that the waters in this part of the study area are under
449 387 the influence of ion exchange and saline intrusion.

450 388 For further confirmation that the ion exchange process affects the hydrochemistry of Remila
451 389 groundwater, another diagram is generated, this diagram has been widely used in various
452 390 studies [BEKKOUSSA *et al.* 2013; KRAIEM 2015]. The diagram $(\text{Ca}^{2+}+\text{Mg}^{2+})-(\text{HCO}_3^-$
453 391 $+\text{SO}_4^{2-})$ versus $(\text{Na}^++\text{K}^+)-\text{Cl}^-$ in (meq.l^{-1}) (Fig. 8(b)) shows that the ion exchange process may
454 392 be a feature of the study area, since most water points follow a straight line ($R^2 = 0.72$) with a
455 393 slope of 1.08, suggesting that the cations Ca^{2+} , Mg^{2+} , Na^+ , and K^+ are integrated into the
456 394 cation exchange reactions. Sample distribution indicates that the most saline groundwater in

the western part of the area has migrated in a direction that is characterized by a rise in Ca^{2+} and Mg^{2+} and a decrease in Na^+ and K^+ concentrations, which suggests that the water mineralization is affected by rock dissolution accompanied by ion exchange. Although water points located in the northeast of the area are characterized by a high concentration of sulphate, they show a slight decrease in Ca^{2+} and Mg^{2+} , whereas significant increases in Na^+ and K^+ are observed. Such findings can be explained by the effect of reverse ion exchange, in which Na^+ is released from the substratum and the Ca^{2+} are adsorbed, and this is favored by the saline intrusion of Sabkha waters [APPELO 1994]. These results confirm that two main processes control our water hydrochemistry: the dissolution of evaporitic rocks, and ion exchange.

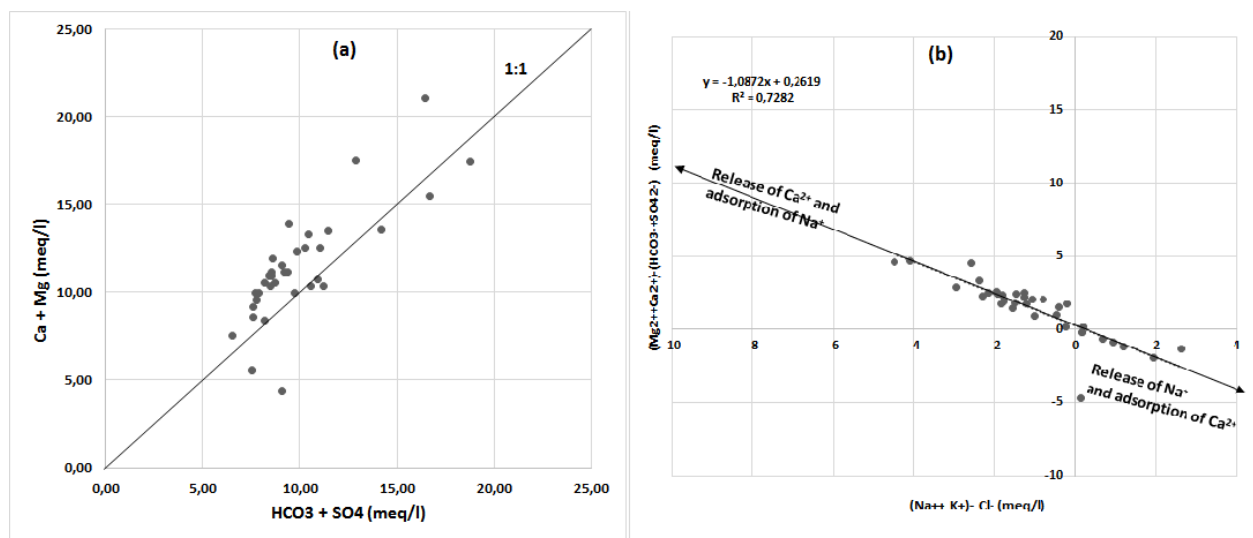


Fig. 8 Scatter plots of a) $(\text{Ca}^{2+} + \text{Mg}^{2+})$ versus $(\text{HCO}_3^- + \text{SO}_4^{2-})$ b) $(\text{Ca}^{2+} + \text{Mg}^{2+}) - (\text{HCO}_3^- + \text{SO}_4^{2-})$ versus $(\text{Na}^+ + \text{K}^+) - \text{Cl}^-$ in (meq.l^{-1}) of the Remila groundwater samples

4 Conclusion

Salinization of water is considered a major problem of land degradation in arid and semi-arid regions. Our research focuses on the endorheic basin of Remila (Khenchela), which is characterized by a semi-arid climate with low and sporadic rainfall. In the study area, the principal source of drinking and irrigation water is groundwater (Plio-quaternary aquifer). A hydrogeochemical and statistical approach was applied in the context of identifying the various salinization processes and the origin of degradation of the aquifer system in the study area.

The results indicate the predominance of three groundwater facies; $\text{SO}_4\text{-Cl-Ca-Ca}$ salt water located to the northeast of the area, $\text{SO}_4\text{-Cl-Ca-Mg}$ moderately saline water which presents the majority of water points, and the type of good quality $\text{HCO}_3\text{-Ca-Mg}$ found in the south-

483 419 eastern part of the area. The statistical analysis of the measured parameters reveals a normal
484 420 distribution of the data, and the VC indicates a moderate to high spatial variability, and this
485 421 suggests that the parameters measured are mainly affected by environmental factors and more
486 422 or less by anthropogenic activities. As well as significant correlations ($r>0.7$) between the
487 423 elements SO_4^{2-} , Cl^- , Mg^{2+} , Na^+ , Ca^{2+} , Sr^{2+} and the global salinity of water (TDS) were found,
488 424 suggesting a common origin of evaporite dissolution. Three water groups were successfully
489 425 identified using PCA and HCA through multivariate statistical analysis; 1) Saltwater (23%),
490 426 where the $\text{TDS} > 1000 \text{ mg.l}^{-1}$ with a high concentration of SO_4^{2-} , 2) Moderately saline waters
491 427 also present (51%) but with high concentrations of HCO_3^- , 3) The bulk of the waters are
492 428 moderately saline (26%) but with a mixed facies.

493 429 The use of ionic ratios with various binary diagrams further suggests that the geochemical
494 430 processes controlling the Remila aquifer system are; Evaporite dissolution and/or
495 431 precipitation (calcite, gypsum, halite, and dolomite) shall be accompanied by ionic exchange
496 432 and/or reverse ionic exchange. In the northeastern part of the Sabkha is produced as well as a
497 433 saline intrusion of waters, which was favored by intense farmers' exploitation of the aquifer.

498 434 The results of this work can be used as a conceptual platform for future research, and to
499 435 prepare a sustainable development plan in the region take into account the risks caused by
500 436 human activity. For example, groundwater overexploitation can be managed by installing a
501 437 suitable and economical irrigation system with the planting of drought-tolerant species with
502 438 the incorporation of unconventional water into the irrigation system.

503 439 **Acknowledgments**

504 440 The authors warmly thank Mr. Abd Elkarim from hydrochemistry laboratory of the Mantouri
505 441 Constantine University, and also the biological laboratory technicians of the Abbes Laghrour
506 442 Khenchela University. We thank the anonymous reviewers and editor for their great help in
507 443 improving the quality of the manuscript.

508 444 **Conflict of interest**

509 445 This research did not receive any specific grant from funding agencies in the public,
510 446 commercial, or not-for-profit sectors.

511 447 **Reference**

512 448 ABU-ALNAEEM M.F., YUSOFF I., NG T.F., ALIAS Y., RAKSMEY M. 2018. Assessment
513 449 of groundwater salinity and quality in Gaza coastal aquifer, Gaza Strip, Palestine: An
514 450 integrated statistical, geostatistical and hydrogeochemical approaches study. Science
515 451 of the Total Environment 615(2018) p. 972-989.
516 452 Doi.org/10.1016/j.scitotenv.2017.09.320

- 518 453 AHOUSSE E.K., SORO N., KOUASSI A.M., ZADE S.P. 2011. Application des méthodes
519 454 d'analyses statistiques multivariées à l'étude de l'origine des métaux lourds (Cu²⁺,
520 455 Mn²⁺, Zn²⁺ et Pb²⁺) dans les eaux des nappes phréatiques de la ville d'Abidjan. *Int J*
521 456 *Biol Chem Sci* 4(5), October 2010 ISSN 1991-8631 p. 1753-1765.
522 457 Doi:10.4314/ijbcs.v4i5.65537.
- 523 458 AKOUVI A., DRAY M., VIOLETTE S., DE MARSILY G., ZUPPI G.M. 2008. The
524 459 sedimentary coastal basin of Togo: example of a multilayered aquifer still influenced
525 460 by a palaeo-seawater intrusion. *Hydrogeol J.* 16 p. 419-436. Doi 10.1007/s10040-007-
526 461 0246-1
- 527 462 AOUIDANE L. 2017b. Origines de la salinisation des eaux et des sols d'une zone à climat
528 463 semi-aride : Cas de Remila (W. Khenchela). Thèse de Doctorat, Université Mohamed
529 464 Khider Biskra. Novembre (2017) pp. 215.
- 530 465 AOUIDANE L., BELHAMRA M. 2017a. Hydrogeochemical processes in the Plio-quaternary
531 466 Remila aquifer (Khenchela, Algeria). *Journal of African Earth Sciences.* 130 p. 38-47.
532 467 Doi.org/10.1016/j.jafrearsci.2017.03.010
- 533 468 APPELO C.A.J. 1994. Cation and proton exchange, pH variations, and carbonate reactions in
534 469 a freshening aquifer. *Water resources research*, Vol. 30, N 10 p. 2793-2805.
- 535 470 APPELO C.A.J. and POSTMA D. 1996. *Geochemistry, groundwater and pollution.* Balkema,
536 471 Rotterdam, pp. 536.
- 537 472 AYADI Y., MOKADEM N., BESSER H., REDHAOUNIA B., KHELIFI F., HARABI S.,
538 473 NASRI T., HAMED Y. 2018. Statistical and geochemical assessment of groundwater
539 474 quality in Teboursouk area (Northwestern Tunisian Atlas). *Environmental Earth*
540 475 *Sciences* (2018) 77:349. <https://doi.org/10.1007/s12665-018-7523-2>
- 541 476 BEKKOUSSA B., JOURDE H., BATIOU-GUILHE C., MEDDI M., KHALDI A., AZZAZ
542 477 H. 2013. Origine de la salinité et des principaux éléments majeurs des eaux de la
543 478 nappe phréatique de la plaine de Ghriss, Nord-Ouest algérien, *Hydrological Sciences*
544 479 *Journal*, 58:5, p. 1111-1127. Doi: 10.1080/02626667.2013.800639.
- 545 480 BENCHOKROUN T. 2008. Ressources en eau et notions de base. *Revue HTE* N°140.
546 481 Septembre 2008 p. 19-25.
- 547 482 BOUZOURRA H., BOUHLILA R., ELANGO L., SLAMA F., OUSLATI N. 2015.
548 483 Characterization of mechanisms and processes of groundwater salinization in irrigated
549 484 coastal area using statistics, GIS, and hydrogeochemical investigations. *Environ Sci*
550 485 *Pollut Res* (2015) 22: p. 2643-2660. Doi 10.1007/s11356-014-3428-0
- 551 486 BROVELLI A., CARRANZA-DIAZ O., ROSSI L., BARRY D.A. 2011. Design
552 487 methodology accounting for the effects of porous medium heterogeneity on hydraulic
553 488 residence time and biodegradation in horizontal subsurface flow constructed wetlands.
554 489 *Ecol. Eng.* 37 (5). p. 758-770.
- 555 490 C.G.G. 1969. *Prospection Géophysique de la plaine de Remila (Khenchela). Coupes*
556 491 *transversales.* Compagne Générale of Géologie. Direction Département des Travaux
557 492 Publique de Batna. 1969. Pp. 35.
- 558 493 C.P.H. 1977. Proposition de réalisation d'étude et projets d'aménagement hydro agricole de la
559 494 plaine de Remila. Rapport de Consortium Projectum-HIDROESB, Rio de Janeiro
560 495 Janvier (1977). Pp.100.

- 562 496 CAPACCIONIA B., DIDERO M., PALETTA C., DIDERO L. 2005. Saline intrusion and
563 497 refreshing in a multilayer coastal aquifer in the Catania Plain (Sicily, Southern
564 498 Italy): dynamics of degradation processes according to the hydrochemical
565 499 characteristics of groundwaters. *Journal of Hydrology* 307(2005) p. 1-16.
566 500 Doi:10.1016/j.jhydrol.2004.08.037.
- 567 501 CASSARDO C., JONES J.A.A. 2011. Managing water in a changing world. *Water* 3: p. 618-
568 502 628. Doi:10.3390/w3020618
- 569 503 CHANGKAKOTI A., MORTON R.D., GRAY J., YONGE C.J. 1986. Oxygen, hydrogen, and
570 504 carbon isotopic studies of the Great Bear Lake silver deposits, Northwest Territories.
571 505 *Earth Sci. Vol. 23.* p. 1463-1469.
- 572 506 D.H.W.K. 1984. Schéma Directeur de planification et d'aménagement. Services de
573 507 production et d'aménagement. Direction de l'Hydraulique de la Wilaya de Khenchela.
574 508 27.
- 575 509 DAVID L. 1999. User's guide to phreeqc (version 2) a computer program for speciation,
576 510 Batch-reaction, one-dimensional transport, and inverse geochemical calculations. U.S.
577 511 Department of the interior. U.S. Geological Survey. Denver, Colorado 1999. Pp. 327.
578 512 <http://www.xs4all.nl/~appt/index.html>
- 579 513 ELANGO L., KANNAN R., SENTHIL K.M. 2003. Major ion chemistry and identification of
580 514 hydrogeochemical processes of groundwater in a part of Kancheepuram district, Tamil
581 515 Nadu, India. *J Environ Geosci.* 10, p. 157-166.
- 582 516 FARID I., TRABELSI R., ZOUARI K., ABID K., AYACHI M. 2013. Hydrogeochemical
583 517 processes affecting groundwater in an irrigated land in central Tunisia. *Environ Earth*
584 518 *Sci* (2013) 68: p. 1215-1231. Doi 10.1007/s12665-012-1788-7
- 585 519 FRAPE S.K., FRITZ P., MCNUTT R.H. 1984. Water-rock interaction and chemistry of
586 520 groundwaters from the Canadian Shield. *Geochim Cosmochim Acta* 48, p. 1617-1627.
- 587 521 GALVAO A.F., GABRIEL M.R., WALTER S.E., WANG L. 2013. Tests for skewness and
588 522 kurtosis in the one-way error component model. *J Multivar Anal* 122. p. 35-52.
- 589 523 GARRELS R.M., MACKENZIE F.T. 1967. Origin of the compositions of some springs and
590 524 lakes. In: Stumm W (ed) *Equilibrium concepts in natural water systems*, Vol 67.
591 525 American Chemical Society, USA, p. 222-242.
- 592 526 GHABAYEN S.M.S., MCKEE M., KEMBLOWSKI M. 2006. Ionic and isotopic ratios for
593 527 identification of salinity sources and missing data in the Gaza aquifer. *Journal of*
594 528 *Hydrology* 318 p. 360-373. Doi:10.1016/j.jhydrol.2005.06.041
- 595 529 GHESQUIÈRE O., WALTER J., CHESNAUX R., ROULEAU A. 2015. Scenarios of
596 530 groundwater chemical evolution in a region of the Canadian Shield based on
597 531 multivariate statistical analysis. *Journal of Hydrology: Regional Studies* 4 p. 246-266.
598 532 Doi.org/10.1016/j.ejrh.2015.06.004
- 599 533 GIBBS R.J. 1970. Mechanisms controlling world water chemistry. *Science, New Series*, Vol.
600 534 170, No 3962 p. 1088-1090.
- 601 535 GIL-MÁRQUEZ J.M., BARBERÁ J.A., ANDREO B., MUDARRA M. 2017. Geochemical
602 536 evolution of groundwater in an evaporite karst system: Brujuelo area (Jaén, Spain).
603 537 *Procedia Earth and Planetary Science* 17 p. 336-339. Doi:
604 538 10.1016/j.proeps.2016.12.085

- 606 539 HAMZAOUI-AZAZA F., TLILI-ZRELLI B., BOUHLILA R., GUEDDARI M. 2012. An
607 540 integrated statistical methods and modeling minerals-water interaction to identifying
608 541 hydrochemical processes in groundwater in southern Tunisia. *Chemical Speciation and*
609 542 *Bioavailability*, 25(3), p. 165-178.
- 610 543 HASSEN I., HAMZAOUI-AZAZA F., BOUHLILA R. 2016. Application of multivariate
611 544 statistical analysis and hydrochemical and isotopic investigations for evaluation of
612 545 groundwater quality and its suitability for drinking and agriculture purposes: case of
613 546 Oum Ali-Thelepte aquifer, central Tunisia. *Environ Monit Assess* 188, 135.
614 547 <https://doi.org/10.1007/s10661-016-5124-7>
- 615 548 HOSSEINI S.Z., KAPPAS M., BODAGHABADI M.B., CHAHOUKI M.A.Z., KHOJASTEH
616 549 E.R. 2014. Comparison of different geostatistical methods for soil mapping using
617 550 remote sensing and environmental variables in Poshtkouh Rangelands, Iran. *Polish*
618 551 *Journal of Environmental Studies*, 23(3), p. 737-751.
- 619 552 KERRY R., OLIVER M.A. 2007. Determining the effect of asymmetric data on the
620 553 variogram. Underlying asymmetry. *Computers and Geosciences*, 33: p. 1212–1232.
621 554 <https://doi.org/10.1016/j.cageo.2007.05.009>
- 622 555 KHARROUBI A., TLAHIGUE F., AGOUBI B., AZRI C., BOURI S. 2012. Hydrochemical
623 556 and statistical studies of the groundwater salinization in Mediterranean arid zones:
624 557 case of the Jerba coastal aquifer in southeast Tunisia. *Environ Earth Sci.* 67: p. 2089-
625 558 2100. Doi 10.1007/s12665-012-1648-5
- 626 559 KRAIEM Z., ZOUARI K., BENCHEIKH N., AGOUN A., ABIDI B. 2015. Processus de
627 560 minéralisation de la nappe du Plio-Quaternaire dans la plaine de Segui-Zograta (Sud-
628 561 Ouest tunisien). *Hydrological Sciences Journal*, 60 ; 3 p. 534-548.
- 629 562 KUMARI R., SINGH C.K., DATTA P.S., SINGH N., MUKHERJEE S. 2013. Geochemical
630 563 modelling, ionic ratio and GIS based mapping of groundwater salinity and assessment
631 564 of governing processes in Northern Gujarat, India. *Environ Earth Sci* 69: p. 2377–
632 565 2391. Doi 10.1007/s12665-012-2067-3.
- 633 566 LAFFITTE R. 1939. Étude géologique de l'Aurès. *Bull Serv Géol de L'Algérie*. 1^o série.
- 634 567 MASOUD A.A., EL-HORINY M.M., ATWIA M.G., GEMAIL K.S., KOIKE K. 2018.
635 568 Assessment of groundwater and soil quality degradation using multivariate and
636 569 geostatistical analyses, Dakhla Oasis, Egypt. *Journal of African Earth Sciences* 142: p.
637 570 64-81. Doi.org/10.1016/j.jafrearsci.2018.03.009
- 638 571 OLIVER M.A. 2010. *Geostatistical Applications for Precision Agriculture*. Springer
639 572 Dordrecht Heidelberg London New York. ISBN 978-90-481-9132-1 pp. 337. DOI
640 573 10.1007/978-90-481-9133-8
- 641 574 OLIVER M.A., LOVELAND P.J., FROGBROOK Z.L., WEBSTER R., MCGRATH S.P.
642 575 2002. Statistical and geostatistical analysis of the national soil inventory of England
643 576 and Wales (MAFF project SPO124, available on CD ROM from National Soil
644 577 Resources Institute, Cranfield University, UK).
- 645 578 OLIVIER A. 2015. *Chimie et pollution des eaux souterraines*. Edition ©Lavoisier, Paris. Pp.
646 579 448. ISBN: 978-2-7430-2009-5
- 647 580 PAZAND K., HEZARKHANI A., GHANBARI Y., AGHAVALI N. 2012. Geochemical and
648 581 quality assessment of groundwater of MarandBasin, East Azarbaijan Province,

- 650 582 northwestern Iran. *Environ Earth Sci* 67. p. 1131-1143. Doi:10.1007/s12665-012-
651 583 1557-7.
- 652 584 PEJMAN A.H., NABI BIDHENDI G.R., KARBASSI A.R., MEHRDADI N., ESMAEILI
653 585 BIDHENDI M. 2009. Evaluation of spatial and seasonal variations in surface water
654 586 quality using multivariate statistical techniques. *Int. J. Environ. Sci. Tech.*, 6 (3), p.
655 587 467-476.
- 656 588 PIPER A.M. 1944. A graphic procedure in the geochemical interpretation of water analyses.
657 589 *Transactions of the American Geophysical Union*, 25. p. 914-923.
- 658 590 PISINARAS V., TSIHRINTZIS V.A., PETALAS C., OUZOUNIS K. 2010. Soil salinization
659 591 in the agricultural lands of Rhodope District, northeastern Greece. *Environ. Monit.*
660 592 *Assess.* 166, p. 79-94.
- 661 593 PLUMMER L.N. 1976. WATEQF, a Fortran IV version of WATEQ, a computer program for
662 594 calculating chemical equilibrium of natural waters. US Geological Survey Water
663 595 Resources Investigation Report p. 76-13. Available from:
664 596 <http://pubdupws.nrc.gov/docs/ML0331/ML033170395.pdf>
- 665 597 RINA K., SINGH C.K., DATTA P.S., SINGH N., MUKHERJEE S. 2013. Geochemical
666 598 modelling, ionic ratio and GIS based mapping of groundwater salinity and assessment
667 599 of governing processes in Northern Gujarat, India. *Environ Earth Sci.* 69: p. 2377-
668 600 2391. Doi:10.1007/s12665-012-2067-3
- 669 601 RODIER J., LEGUBE B., MERLET N. 2016. *L'analyse de l'eau*. 10e édition entièrement.
670 602 Paris : Dunod - DL. Pp. 867.
- 671 603 SANCHEZ-MARTOS F., PULIDO-BOSCH A., MOLINA-SANCHEZ L., VALLEJOS-
672 604 IZQUIERDO A. 2002. Identification of the origin of salinization in groundwater using
673 605 minor ions (Lower Andarax, Southeast Spain). *The Science of the Total Environment*
674 606 297. p. 43-58.
- 675 607 SCANLON B.R., KEESE K.E., FLINT A.L., FLINT L.E., GAYE C.B., EDMUND W.M.,
676 608 SIMMERS I. 2006. Global synthesis of groundwater recharge in semiarid and arid
677 609 regions. *Hydrol. Process.* 20 p. 3335-3370. Doi: 10.1002/hyp.6335
- 678 610 SIEBERT S., BURKE J., FAURES J.M., FRENKEN K., HOOGEVEEN J., DOLL P.,
679 611 PORTMANN F.T. 2010. Groundwater use for irrigation a global inventory. *Hydrol*
680 612 *Earth Syst Sci*, 14, p. 1863-1880.
- 681 613 SINGH C.K., KUMAR A., SHASHTRI S., KUMAR A., KUMAR P., MALLICK J., 2017.
682 614 Multivariate statistical analysis and Geochemical modeling for geochemical
683 615 assessment of groundwater of Delhi, India. *Journal of Geochemical Exploration.* 175,
684 616 p. 59-71. <https://doi.org/10.1016/j.gexplo.2017.01.001>
- 685 617 SINGH K., HUNDAL H.S., SINGH D. 2011. Geochemistry and assessment of
686 618 hydrogeochemical processes in groundwater in the southern part of Bathinda district
687 619 of Punjab, northwest India. *Environ Earth Sci.* 64. p. 1823-1833.
- 688 620 SRINIVASAMOORTHY K., GOPINATH M., CHIDAMBARAM S., VASANTHAVIGAR
689 621 M., SARMA V.S. 2014. Hydrochemical characterization and quality appraisal of
690 622 groundwater from Pungar sub basin, Tamilnadu, India. *Journal of King Saud*
691 623 *University-Science.* 26, p. 37-52. Doi.org/10.1016/j.jksus.2013.08.001
- 692 624 SUDHEER K.M., RATNAKAR D., YADAGIRI G., SRINIVASA R.K. 2017. Pincipal
693 625 component and multivariate statistical approach for evaluation of hydrochemical

- 695 626 characterization of fluoride-rich groundwater of Shaslar Vagu watershed, Nalgonda
696 627 District, India. Arab J Geosci. 10: 83. Doi:10.1007/s12517-017-2863-x
- 697 628 TIJANI M.N. 2004. Evolution of saline waters and brines in the Benue-Trough, Nigeria.
698 629 Applied Geochemistry 19(9): p. 1355-1365. Doi:10.1016/j.apgeochem.2004.01.020.
- 699 630 TLILI-ZRELLI B., HAMZAOUI-AZAZA F., GUEDDARI M., BOUHLILA R. 2013.
700 631 Geochemistry and quality assessment of groundwater using graphical and multivariate
701 632 statistical methods. A case study: Grombalia phreatic aquifer (northeastern Tunisia).
702 633 Arabian Journal of Geosciences, 6, p. 3545-3561.
- 703 634 VAN BREUKELEN B.M., APPELO C.A.J., OLSTHOORN T.N. 1998. Hydrogeochemical
704 635 transport modeling of 24 years of Rhine water infiltration in the dunes of the
705 636 Amsterdam Water Supply. Journal of Hydrology. 209, (1-4): p. 281-296.
706 637 [https://doi.org/10.1016/S0022-1694\(98\)00105-X](https://doi.org/10.1016/S0022-1694(98)00105-X)
- 707 638 VAROL S., DAVRAZ A. 2014. Assessment of geochemistry and hydrogeochemical
708 639 processes in groundwater of the Tefenni plain (Burdur/Turkey). Jor Environ Earth Sci.
709 640 71. p. 4657-4673.
- 710 641 VILA J.M. 1977. Notice explicative de la carte géologique, au 1/50.000, Touffana (feuille n°
711 642 202). Editée par Sonatrach en 1977, Algérie. Pp. 6.
- 712 643 VISWANATH N.C., KUMAR P.G.D., AMMAD K.K. 2015. Statistical Analysis of Quality
713 644 of Water in Various Water Shed for Kozhikode City, Kerala, India. Aquatic Procedia.
714 645 4: p. 1078-1085. Doi:10.1016/j.aqpro.2015.02.136.
- 715 646 WALTON W.C. 1965. Groundwater recharge and runoff in Illinois. Illinois State Water
716 647 Surv., Rept. Of Invest. Pp. 48.
- 717 648 WANG Y., JIAO J.J. 2012. Origin of groundwater salinity and hydrogeochemical processes
718 649 in the confined Quaternary aquifer of the Pearl River Delta, China. Journal of
719 650 Hydrology 438–439 : p. 112-124. Doi: 10.1016/j.jhydrol.2012.03.008.
- 720 651 YANG F., ZHANG G., YIN X., LIU Z. 2011. Field-Scale Spatial Variation of Saline-Sodic
721 652 Soil and Its Relation with Environmental Factors in Western Songnen Plain of China.
722 653 Int. J. Environ. Res. Public Health. 8, p. 374-387. Doi:10.3390/ijerph8020374.
- 723 654 YERMANI M., ZOUARI K., MICHELOT J.L., MAMOUCHE A., MOUMNI L. 2003. Approche
724 655 géochimique du fonctionnement de la nappe profonde de Gafsa Nord (Tunisie
725 656 centrale). Hydrological Sciences Journal, 48:1 p. 95-108. Doi:
726 657 10.1623/hysj.48.1.95.43482
- 727 658 YIDANA S.M., OPHORO D., BANOENG-YAKUBO B. 2008. A multivariate statistical
728 659 analysis of surface water chemistry data the Ankobra Basin, Ghana. Journal of
729 660 Environmental Management, 86: p. 80-87.
- 730 661 ZEKTSER I.S., EVERETT L.G. 2004. Resources of the word and their use. UNESCO 2004,
731 662 75352. Paris 07 SP. ISBN 92-9220-007-0. Pp. 342.
- 732 663 ZEWDU S., SURYABHAGAVAN K.V., BALAKRISHNAN M. 2017. Geo-spatial approach
733 664 for soil salinity mapping in Sege Irrigation Farm, South Ethiopia. Journal of the Saudi
734 665 Society of Agricultural Sciences. 16, p. 16-24. Doi.org/10.1016/j.jssas.2014.12.003.

Tables:**Table 1.** Methods used for major ion and isotope analysis in the waters of Remila

Elements	Methods of analysis
Ca ²⁺ and Na ⁺	Industrial flame photometers PFP7
Mg ²⁺ , K ⁺ , Sr ²⁺ , Al ²⁺ and Li ⁺	Perkin Elmer atomic absorption AA 200 (FXAA)
SO ₄ ²⁻ and NO ₃ ⁻	Colorimetric method
Cl ⁻ and HCO ₃ ⁻	Volumetric method

Table 2. Descriptive statistics of Remila water parameters (mg/l)

	campaign	Mean	Median	Minimum	Maximum	Std.Dev.	Coef.Var.	Skewness	Kurtosis
pH	2013	6.87	6.92	6.52	7.02	0.13	1.90	-1.51	1.33
	2014	6.91	6.92	6.50	7.21	0.11	1.55	-1.27	7.09
TDS	2013	896.29	824.50	568.00	1586.00	254.52	28.40	1.29	1.13
	2014	1797.14	1710.00	1250.00	3270.00	485.57	27.02	1.67	2.87
Ca ²⁺	2013	134.74	132.26	40.08	252.50	39.36	29.21	0.49	2.41
	2014	132.14	128.26	44.09	248.50	46.42	35.13	0.76	1.18
Mg ²⁺	2013	50.83	35.88	6.96	239.64	53.54	105.34	2.63	6.50
	2014	56.83	52.68	28.80	129.48	22.48	39.55	2.04	4.59
Na ⁺	2013	55.56	41.75	11.96	145.59	34.78	62.61	1.45	1.49
	2014	69.46	62.11	29.67	162.15	33.45	48.16	0.93	0.41
K ⁺	2013	1.09	0.17	0.02	9.98	2.09	191.45	2.94	9.57
	2014	1.16	1.00	0.09	3.95	0.80	69.13	1.87	4.43
HCO ₃ ⁻	2013	174.75	164.70	54.90	280.60	53.64	30.70	0.31	-0.30
	2014	253.20	256.20	183.00	402.60	48.86	19.30	0.96	1.39
Cl ⁻	2013	122.80	118.93	35.50	312.40	58.36	47.53	1.16	2.07
	2014	125.79	117.15	35.50	333.70	83.41	66.31	1.22	0.90
SO ₄ ²⁻	2013	344.24	320.00	160.00	704.00	129.92	37.74	1.64	2.84
	2014	293.86	270.00	140.00	1250.00	188.44	64.13	4.05	20.20
NO ₃ ⁻	2013	-	-	-	-	-	-	-	-
	2014	8.19	3.60	0.20	39.00	11.09	135.45	1.96	2.42

Std.Dev: Standard Deviation; Coef.Var: Coefficient of variation.

Table 3. Correlation matrix of different water parameters in the Remila plain (Khenchela) (mg/l)

Variable	pH	TDS	Ca	Mg	Na	K	HCO ₃	Cl	SO ₄	Fe	Mn	Sr
pH	1.00											
TDS	0.16	1.00										
Ca	0.22	<u>0.66</u>	1.00									
Mg	0.26	<u>0.87</u>	0.43	1.00								
Na	0.00	<u>0.81</u>	0.17	<u>0.69</u>	1.00							
K	0.16	<u>0.82</u>	0.38	<u>0.79</u>	<u>0.75</u>	1.00						
HCO ₃	-0.33	0.20	-0.14	-0.02	0.44	0.14	1.00					
Cl	0.31	<u>0.81</u>	<u>0.74</u>	<u>0.68</u>	<u>0.55</u>	<u>0.65</u>	-0.18	1.00				
SO ₄	0.19	<u>0.96</u>	<u>0.61</u>	<u>0.93</u>	<u>0.74</u>	<u>0.80</u>	0.02	<u>0.73</u>	1.00			
Fe	-0.08	0.21	0.28	0.15	0.00	0.20	0.08	0.16	0.20	1.00		
Mn	0.01	-0.24	-0.36	-0.21	-0.05	-0.12	0.24	-0.44	-0.22	-0.07	1.00	
Sr	-0.01	<u>0.71</u>	<u>0.58</u>	<u>0.57</u>	0.45	0.62	0.34	0.46	<u>0.66</u>	0.36	-0.04	1.00

Table 4. Varimax factor loading matrix, communalities for each variable analyzed

Parameters	Factor 1	Factor 2	Factor 3	Factor 4	Factor 5
pH	-0.2245	-0.5564	0.4408	0.1886	-0.2360
TDS	-0.9795	0.0831	0.0054	-0.0857	0.0711
Ca	-0.6711	-0.3059	-0.4608	0.0097	-0.2072
Mg	-0.8954	-0.0599	0.2170	0.0042	0.0861
Na	-0.7563	0.3892	0.3325	-0.1522	0.2471
K	-0.8628	0.1267	0.1683	-0.0418	0.0688
HCO ₃	-0.0889	0.8501	-0.0524	-0.0639	0.2252
Cl	-0.8338	-0.3110	-0.0842	-0.0693	-0.0157
SO ₄	-0.9552	-0.0205	0.0742	-0.0525	0.0339
Fe	-0.2704	0.0499	-0.5723	0.5659	0.1012
Mn	0.2749	0.4881	0.4029	0.2935	-0.3649
Sr	-0.7282	0.3298	-0.3126	0.1030	-0.1388

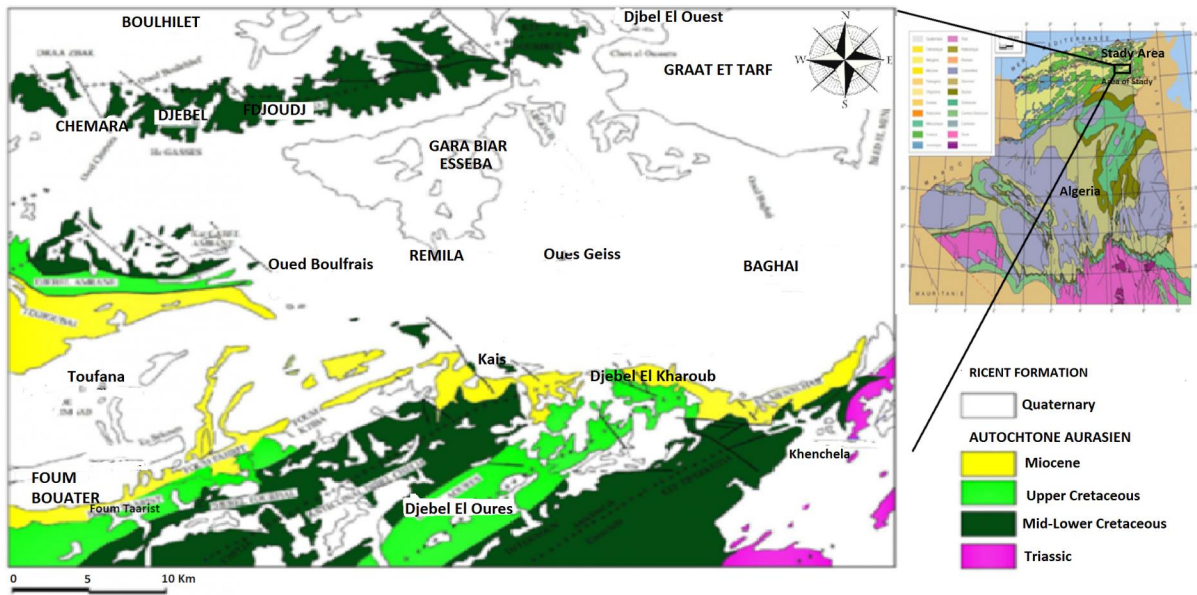


Fig. 1. Map showing location and geological formations of the study area

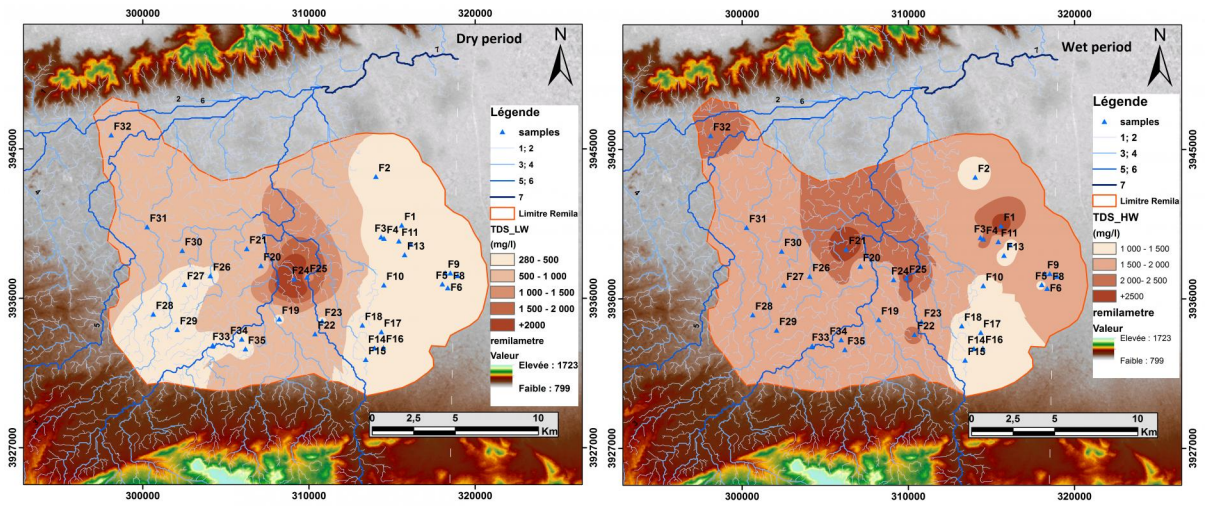


Fig. 2. Spatial salinity distribution map (TDS) of groundwater Remila (Khenchela)

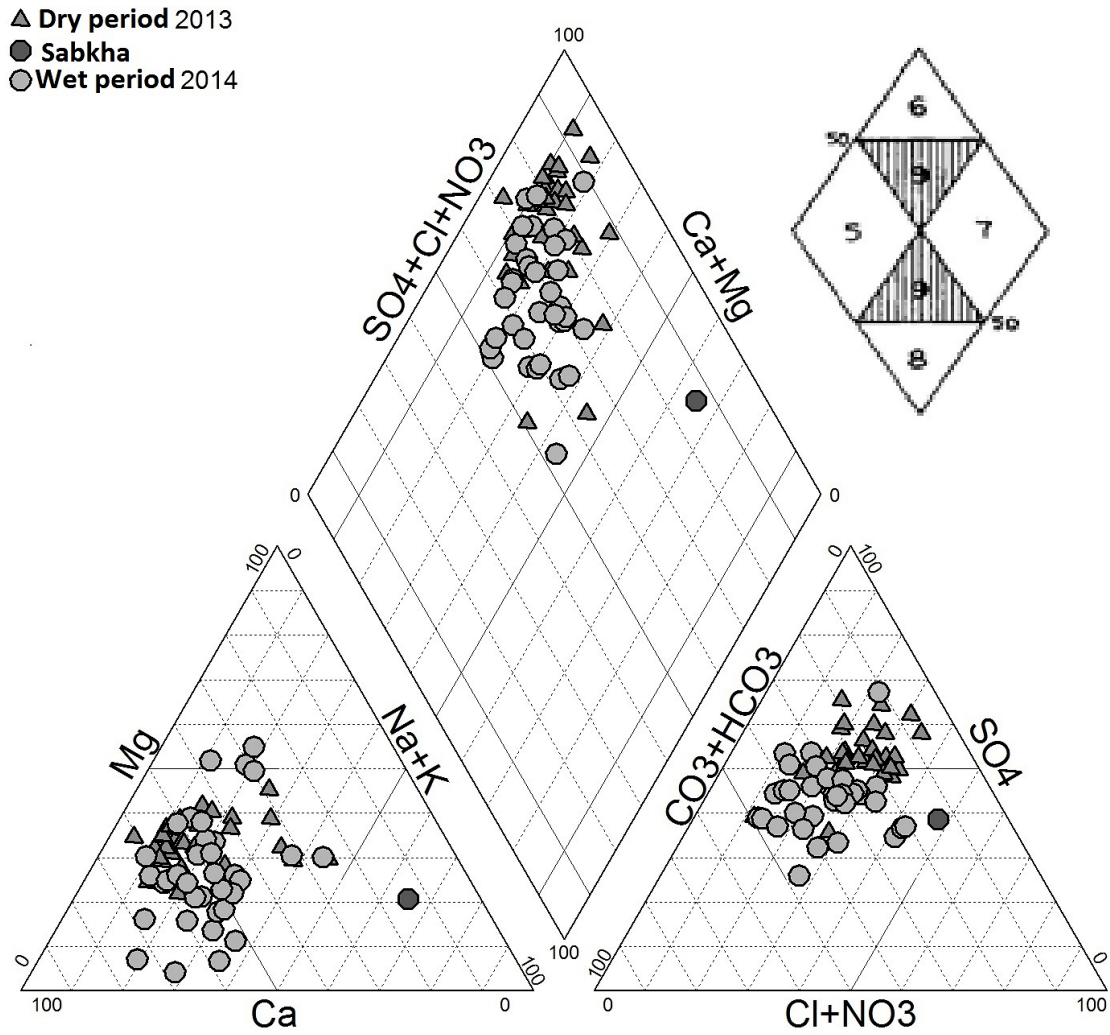


Fig. 3. Piper diagram of Remila groundwater (Dry period and Wet period).

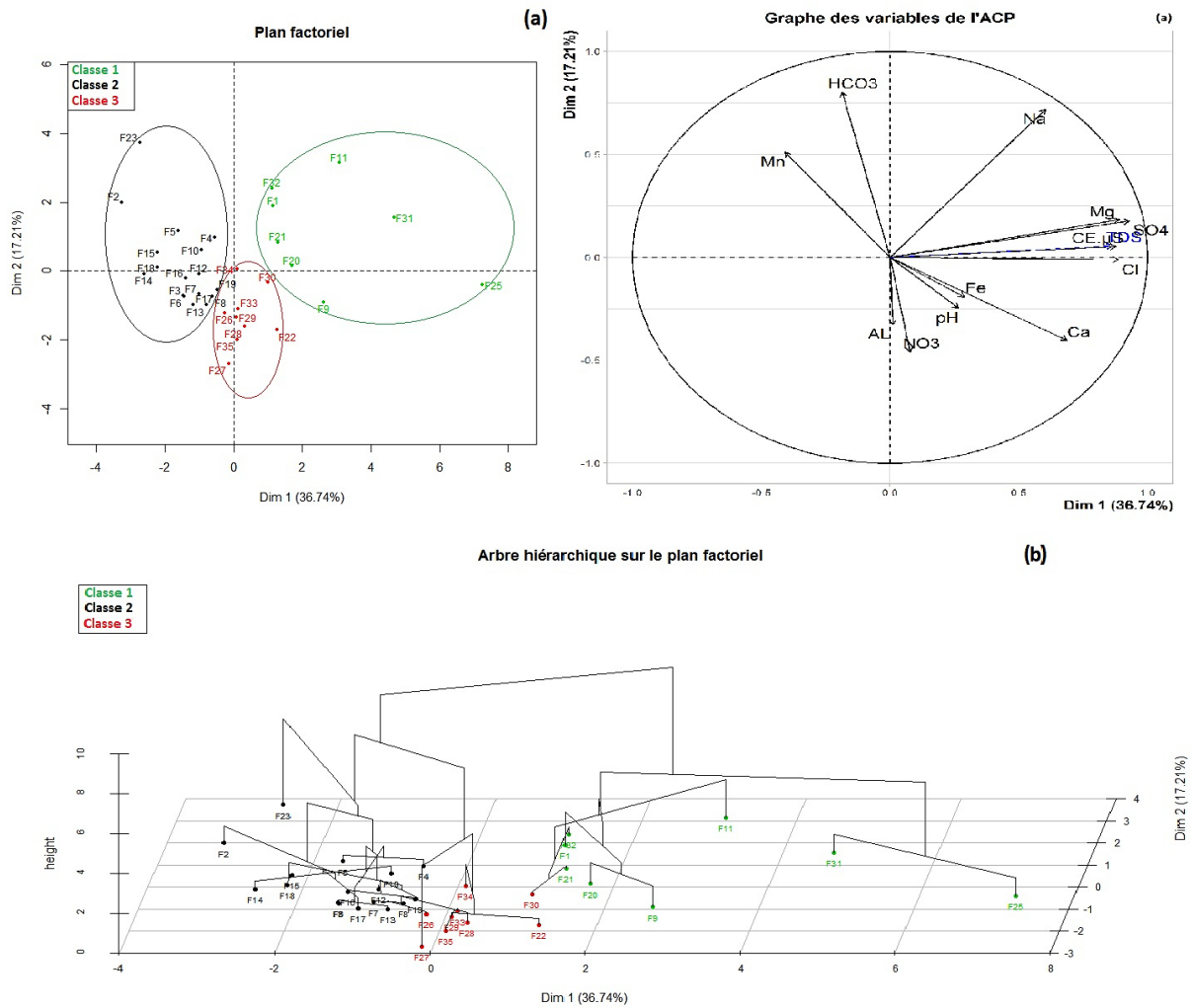


Fig. 4. Statistic analysis; (a) Principal component analysis, (b) the Ascending hierarchical clustering of Remila waters (Khenchela)

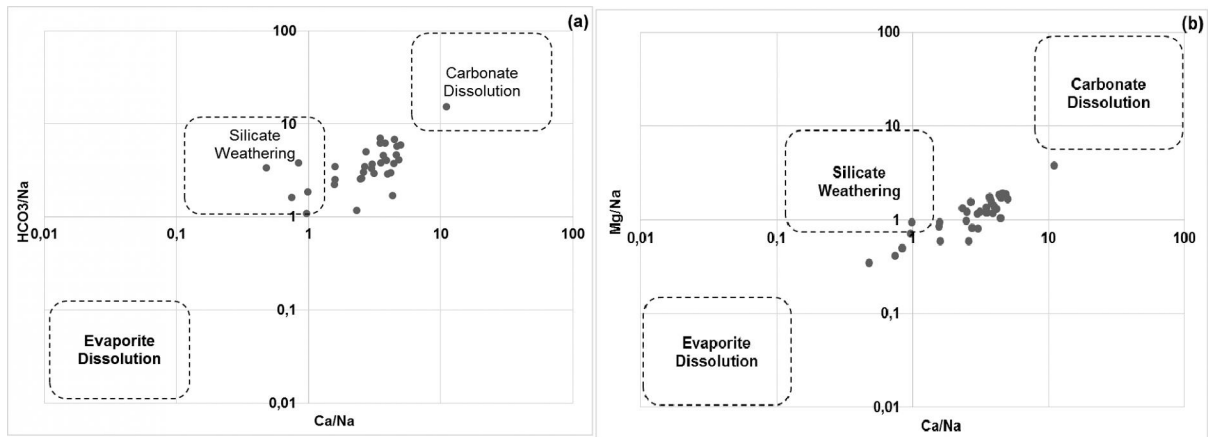


Fig. 5. Scatter plots of a) $\text{Ca}^{2+}/\text{Na}^{+}$ versus $\text{HCO}_3^{-}/\text{Na}^{+}$, b) $\text{Ca}^{2+}/\text{Na}^{+}$ versus $\text{Mg}^{2+}/\text{Na}^{+}$ ration of the Remila groundwater samples

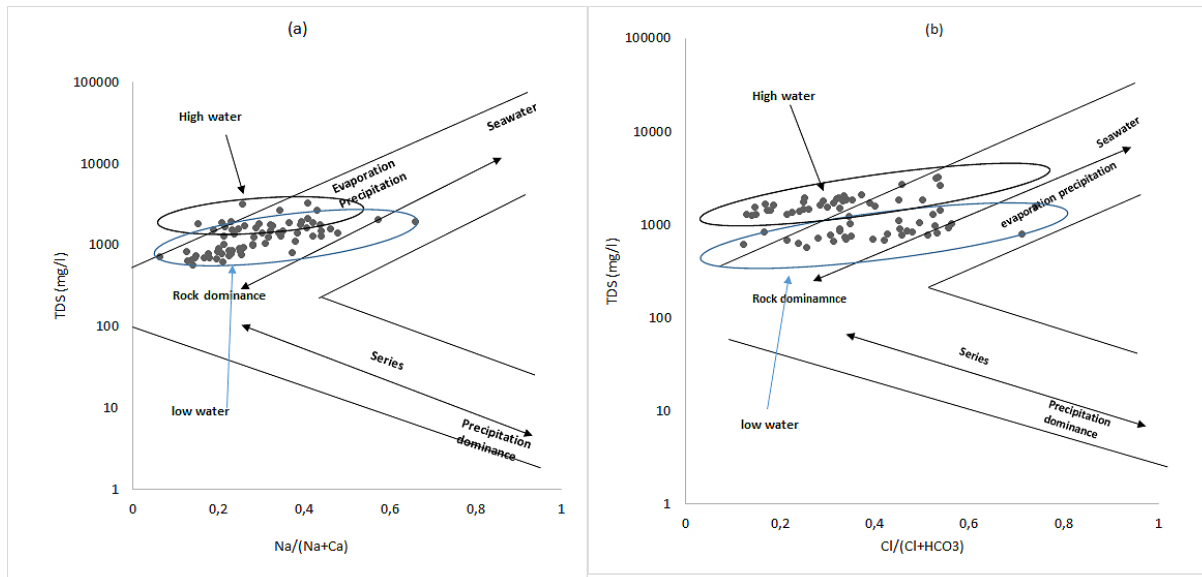


Fig. 6. Gibbs diagrams of Remila groundwater

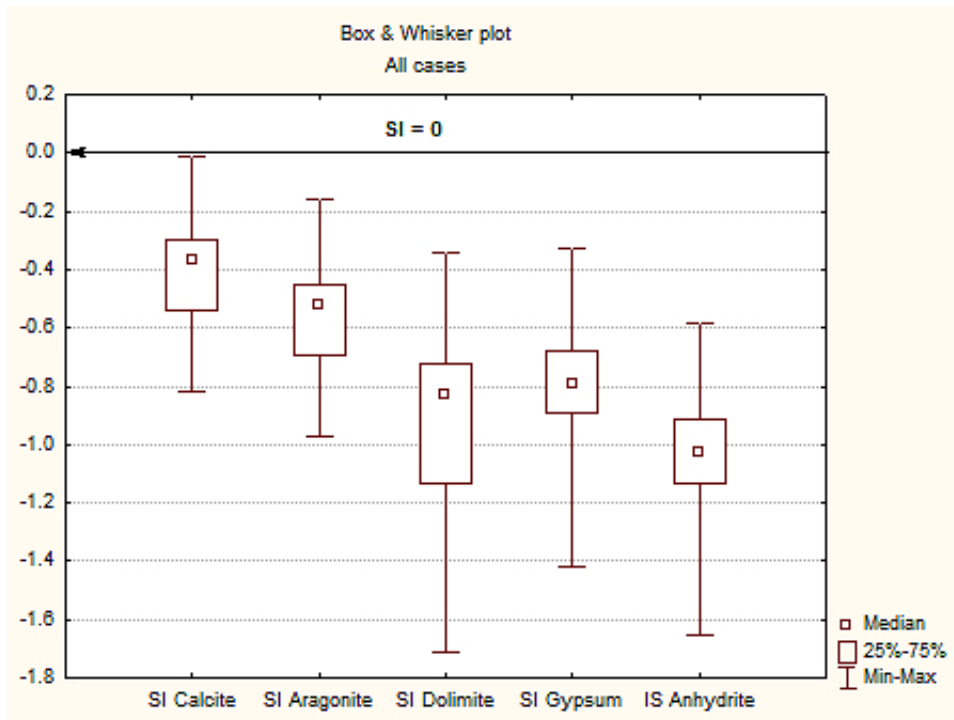


Fig. 7. Saturation index (SI) variability diagrams in groundwater at Remila (Khenchela)

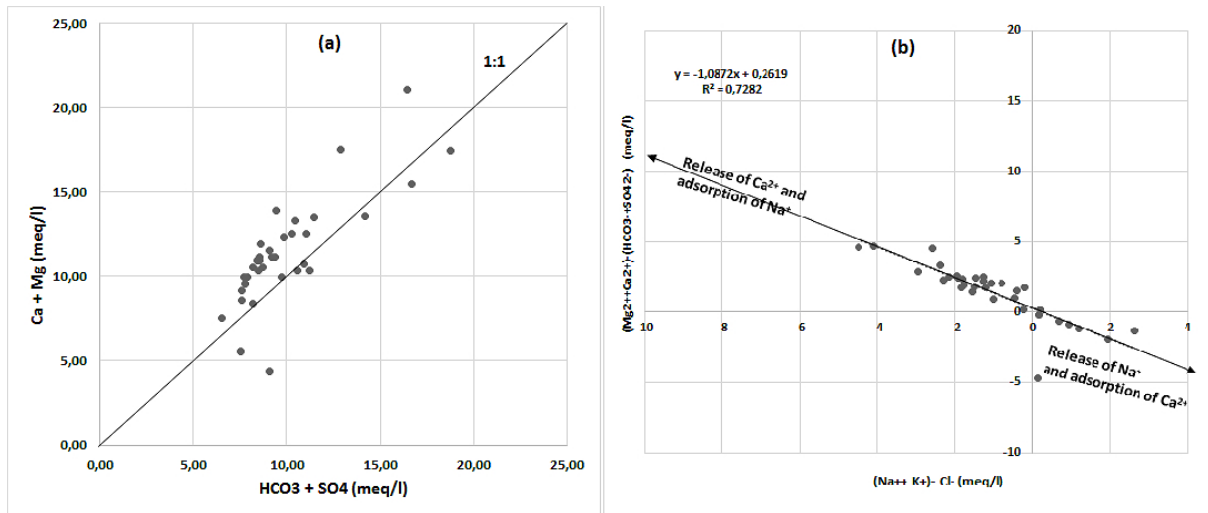


Fig. 8. Scatter plots of a) $(\text{Ca}^{2+} + \text{Mg}^{2+})$ versus $(\text{HCO}_3^- + \text{SO}_4^{2-})$ b) $(\text{Ca}^{2+} + \text{Mg}^{2+}) - (\text{HCO}_3^- + \text{SO}_4^{2-})$ versus $(\text{Na}^+ + \text{K}^+) - \text{Cl}^-$ in (meq/l) of the Remila groundwater samples

Manuscript body

[Download source file \(11.23 MB\)](#)

Tables

[Download source file \(102 kB\)](#)

four tables

Figures

Figure 1 - [Download source file \(2.49 MB\)](#)

Fig. 1. Map showing location and geological formations of the study area

Figure 2 - [Download source file \(11.74 MB\)](#)

Fig. 2. Spatial salinity distribution map (TDS) of groundwater Remila (Khenchela)

Figure 3 - [Download source file \(441.61 kB\)](#)

Fig. 3. Piper diagram of Remila groundwater (Dry period and Wet period).

Figure 4 - [Download source file \(253.23 kB\)](#)

Fig. 4. Statistic analysis; (a) Principal component analysis, (b) the Ascending hierarchical clustering of Remila waters (Khenchela)

Figure 5 - [Download source file \(78.71 kB\)](#)

Fig. 5. Scatter plots of a) $\text{Ca}^{2+}/\text{Na}^{+}$ versus $\text{HCO}_3^{-}/\text{Na}^{+}$, b) $\text{Ca}^{2+}/\text{Na}^{+}$ versus $\text{Mg}^{2+}/\text{Na}^{+}$ ration of the Remila groundwater samples

Figure 6 - [Download source file \(159.44 kB\)](#)

Fig. 6. Gibbs diagrams of Remila groundwater

Figure 7 - [Download source file \(17.21 kB\)](#)

Fig. 7. Saturation index (SI) variability diagrams in groundwater at Remila (Khenchela)

Figure 8 - [Download source file \(138.05 kB\)](#)

Fig. 8. Scatter plots of a) $(\text{Ca}^{2+}+\text{Mg}^{2+})$ versus $(\text{HCO}_3^{-} + \text{SO}_4^{2-})$ b) $(\text{Ca}^{2+}+\text{Mg}^{2+})-(\text{HCO}_3^{-}+\text{SO}_4^{2-})$ versus $(\text{Na}^{+}+\text{K}^{+})-\text{Cl}^{-}$ in (meq/l) of the Remila groundwater samples